The study of the effect of microcontractions in the separation of blood cells: soft lithography and micromilling.

Ana Raquel Jácome Lopes

Final Project Report to the **Escola Superior de Tecnologia e Gestão**
Instituto Politécnico de Bragança
To obtain Master degree in **Tecnologia Biomédica**

November 2014

INSTITUTO POLITÉCNICO DE BRAGANÇA
Escola Superior de Tecnologia e Gestão

The study of the effect of microcontrations in the separation of blood cells: soft lithography and micromilling.

Ana Raquel Jácome Lopes

Final Project Report to the Escola Superior de Tecnologia e Gestão
Instituto Politécnico de Bragança
To obtain Master degree in **Tecnologia Biomédica**

Advisors:
Rui Lima
Stefan Gaβmann

"This is the Final Project Report which include the critiques and suggestions from the Jury"

This Final Project Report was a collaboration of Jade Hochschule

November 2014

“Learn from yesterday, live for today, hope for tomorrow.
The important thing is not stop questioning.”
Albert Einstein

Acknowledgments

The author acknowledge the support provided by: Student Mobility Placements with the program Lifelong Learning (Erasmus Program), PTDC/SAU-ENB/116929/2010, EXPL/EMS-SIS/2215/2013 from the FCT (Science and Technology Foundation), QREN, European Union (FEDER) and COMPETE, Portugal and to the Polytechnic Institute of Bragança that assigned the scholarship for the elaboration of master thesis with cooperation of Jade Hochschule, Wilhelmshaven, Germany.

I'm grateful to:

To my advisors and co-advisors, Rui Lima, Stefan Gaβmann, Valdemar Garcia and Patricia Sousa, all the support and knowledge that they share with me.

To MsC Diana Pinho, Raquel Rodrigues, Vera Faustino and Professor Helmut Shütte for the patient and all knowledge they shared with me.

To my Parents, Sisters, cousins and uncles for the trust, the support, without them this couldn't be possible, especially to my grandmother Lucinda Dias and my untie Clara Lopes for giving me this opportunity.

To Marco Leite for insisting every day for me to work and for being there every time I needed.

And to all my friends for helping with my moments of stress and for not letting me give up.

Abstract:

The detection, separation and manipulation of microparticles and blood cells are important stages for biologic and chemical analysis. A new application in the area of Biomedical Engineering with potential is the development of portables micro devices for diagnostic, those are known as lab-on-chips or blood-on-chips. Their principal function is the separation and identification pathological cells in a blood sample. For example, infected cells with diabetes and malaria, present different deformation indices from healthy ones. This device should be a simple and low cost way to separate pathologic cells from healthy. The goal of this work is to design a geometry containing a microcontraction and test its effect in the cell free layer (CFL) and consequently in the separation of cells from plasma.

In a first phase, it is used a soft lithography method for the fabrication of hyperbolic microchannels in PDMS. The hyperbolic microchannels are tested with a hematocrit of 5% of ovine red blood cells. Some results were presented and discussed.

A low cost fabrication method was used, consisting in using a micromilling machine to mill in PMMA glass or Plexiglass to fabricate microchannels with simple contractions. The microchannels were tested with 5% of ovine red blood cells. The low cost method was discussed and some results about cell separation were presented.

Keywords: Biomedical devices, lab-on-chips, micromilling, Lithography, cell free layer

Resumo:

A deteção, separação e manipulação de micropartículas e células sanguíneas são fases importantes para uma análise química e biológica. Uma nova aplicação na área de Engenharia Biomédica com potencial é o desenvolvimento de microdispositivos portáteis para diagnóstico, mais conhecidos como “lab-on-chips” ou “blood-on-chips”.

A principal função destes dispositivos é a separação e identificação de células patológicas numa amostra de sangue. Certas doenças como a diabetes e a malaria alteram os índices de deformação dos Glóbulos vermelhos, sendo o objetivo deste dispositivo a separação das células saudáveis das patológicas de uma maneira simples e barata. O objetivo deste trabalho é projetar uma geometria com uma microcontração e testar o efeito na camada livre de célula e consequentemente a sua eficácia na separação de células do plasma.

Numa primeira fase é realizada uma pequena explicação sobre litografia, assim como os resultados e discussão dos escoamentos com sangue dos canais produzidos em PDMS a partir de um molde em uma *wafer* feitos por litografia com SU8.

Numa segunda fase é explicado brevemente o processo de produzir microcanais, com uma micro-fresadora, em vidro de PMMA. Este processo consistiu em desenhar a geometria, o manuseamento dos *softwares* e os acabamentos finais nos microcanais fabricados.

Palavras-chave: Dispositivos biomédicos, lab-o-chips, Micro-fresadora Litografia, camada livre de células.

Table of contents

List of figures

List of tables

List of abbreviations

2D – two dimensional/dimension

3D – three dimensional/dimension

PDMS – Poly (dimethylsiloxane)

CFL – Cell Free Layer

RBCs – red blood cells

WBCs – white blood cells

SEM – Scanning electron microscopy

UV – ultraviolet

Chapter I - Introduction

1. Objectives and motivation

A rapidly emerging field in lab-on-a-chip research is the development of devices to improve the health of people in developing countries, since the resources are scarce. The principal function of the produced device is the separation and identification of pathological cells in a blood sample. This can help finding a disease before it becomes critical, for example, malaria that kills thousands of people every year. The blood cells infected with malaria are known to be rigid, and rigid cells tend to travel near the vessel wall. By using this phenomenon if it is possible to separate the rigid cells from the healthy cells, they can be analysed and the disease can be detected in earlier stages and maybe prevented. The developed microfluidic device should have a potential for the use for early detection of other types of blood diseases.

One of most popular and traditional method to fabricate microfluidic devices is the soft lithography technique with polydimethylsiloxane (PDMS) structures made from SU-8 molds (Duffy *et al* 1998, Leble *et al* 2011, Lima *et al* 2008). The SU-8 molds are produced by photolithography. The main attraction for this technology is due mainly to its high resolution capabilities, low material cost, gas permeability and optical transparency (Duffy *et al* 1998). However, the production of molds by photolithography usually requires a clean-room environment and specialized equipment that can be quite costly and time consuming. These drawbacks are currently slowing down, specially in research institutions without specialized facilities to produce molds by photolithography.

The main goal of this work is to find a reliable microchannel geometry for the separation of microparticles as well as rigid cells from deformable red blood cells by using alternative methods to the soft-lithography technique. By using micro-milling several microchannels with different geometries were manufactured and tested. Additionally, hyperbolic microchannels fabricated by the traditional soft-lithography technique was also tested.

2. **Structure**

The current work is divided into the following chapters: In Chapter 1 an introduction to the work, concepts and reviews of relevant studies are presented.

In Chapter 2 we refer to biofluidics, where we present the principal concepts, including the hemodynamics; the blood and its composition.

Chapter 3 introduces micro milling technique. We show the process of the construction of the micro devices with a micro milling machine, which consists of the drawing, the milling, and the finishing touches. Then the blood flow analyses and the results are obtained.

In Chapter 4, we provide an introduction to the basics of soft lithography. Then the blood flow experiments on the channels done by lithography are described. Additionally, it is shown the second part of the study done in Germany, which is the study of a positive resist and how to proceed to get better results.

Chapter II – Bio fluidics

3. Introduction

A fluid can be defined as substance that suffers a continuous deformation when submitted to a tangential force. This notion encompasses liquids and gases, which can be distinguished by the degree of compressibility, where liquids are mostly uncompressible contrary to gases, which in a condition of pressure present increased compressibility (Calejo, 2013), (Rosário, et al., 2007).

A bio fluid is a fluid produced by the organism, which means it is all the fluids that exist in biologic systems, as blood, urine, pus, sweat and others (Rosário, et al., 2007), (Calejo, 2013), (Pinho, 2011). As you will develop knowledge about the mechanisms of action of the living beings, the study of the behaviour of bio fluids is getting more interesting, since they are important in the operation of any biologic system (Calejo, 2013).

In the human being the blood is the most important fluid, since it is involved in numerous organisms' functions, contributing to their homeostasis. The blood analysis with laboratory methods give relevant data for diagnosing many pathologies (Calejo, 2013), (Pinho, 2011).

4. Hemodynamics and Blood Circulatory System

The principal functions of the circulating blood is the transportation of oxygen, nutrients, waste products and heat through the body. The blood that reaches the heart from the lungs goes through the entire body, therefore it leaves the heart with high pressure and velocity, with a Reynolds number (Re) bigger than 2000. The oxygenated blood leaves the heart through the aorta and moves into other large arteries, then into arterioles and finally to the capillaries. From the capillaries it goes back to the heart, moving through venules, then the veins in order to do the same journey all over again (Novais, 2012).

In big arteries where the diameter is large enough compared to individual cells, it is possible to consider the blood as a single-phase fluid, which make possible the study of the blood as a homogeneous fluid, ignoring its particular nature. Because of the high

number of Re in the arteries the blood flow is governed by inertial forces (Yamaguchi, et al., 2006).

However, the arteries are divided in continuous arteries with smaller diameter, which results in the amplification of the transversal section and both the pressure and velocity decreases as the blood flows into the smaller vessels, cf. Fig.1 (Fung, 1993 and Yamaguchi, et al., 2006). When the blood reach the arterioles and capillary, Re number becomes less than one and the viscosity forces dominates over the inertial forces. In micro dimensions it is essential to take into account the effect of non-Newtonian proprieties of the blood, for the study of its behaviour in micro-vessels and micro-channels (Novais, 2012).

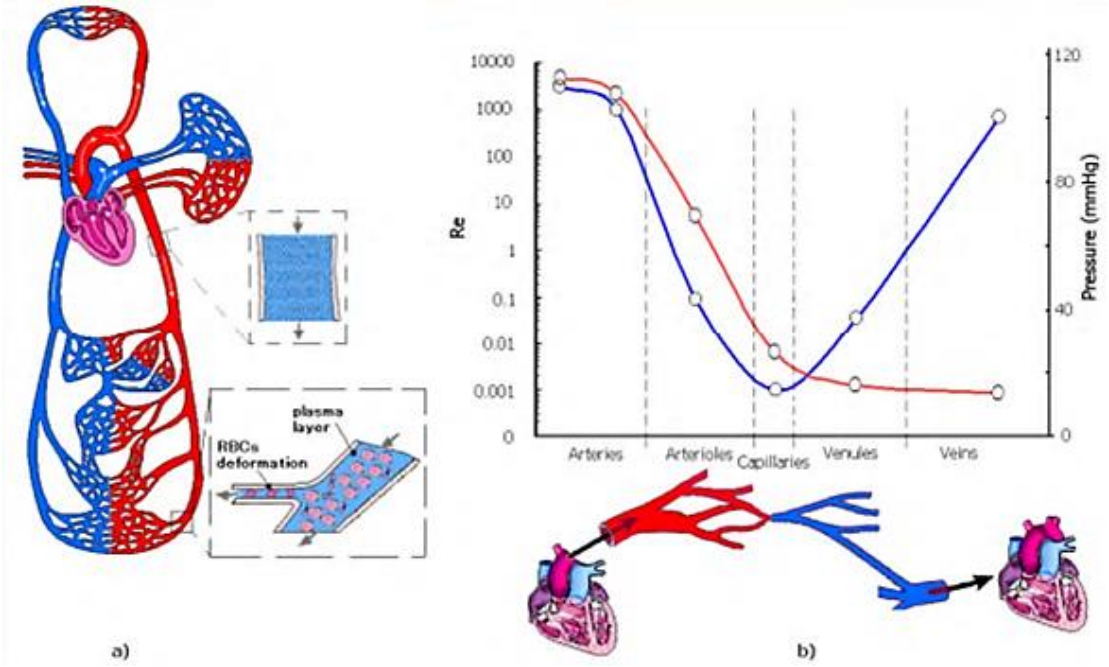

Figure 1 - a) Schematic diagram of the circulatory system. b) Schematic diagram showing the changes in blood pressure and Re on the large arteries, capillaries and veins (Yamaguchi, et al., 2006).

5. **Blood Composition**

The blood is a multiphasic complex fluid that transports the vital substances for the cell tissues and human organs. It consists of a suspension of cellular elements like red blood cells (RBCs), white blood cells (WBCs), and platelets, in an aqueous matrix of molecules, organic proteins and salts called plasma (Novais, 2012).

The blood is an opaque fluid, with a viscosity higher than water. It is heterogeneous consisting of a clear liquid, the plasma and a set of various cellular

elements. The blood is in a closed compartment, the circulatory system which keeps it in an unidirectional flow. In an adult with 70Kg, the blood is 7% of the human weight or about 5 litters in which 60% is plasma. The volume of red blood cells in the blood is called haematocrit, which is normally 45% for men and 40% for women (Novais, 2012).

Red blood Cells (RBC)

Red blood cells, also called erythrocytes are 700 times more numerous than the WBCs and 17 times more than the platelets and are moved by the forces of the circulatory system. The size of the RBC varies with diameter between 5 µm and 8 µm which originates some effects that should be considered in the microfluidic simulation. (Novais, 2012)

The function of the RBC is the transportation of the oxygen from the lungs to the various tissues in the human organism and the CO_2 to the lungs. This transport is executed by the haemoglobin, which is 25% of the volume of the erythrocyte.

In the absence of stress applied in the blood, the RBC's present themselves as biconcave discs with a diameter of about 7.5 µm (Figure 2). the biconcave shape increases the superficial area of the RBC, making the entrance and exit of the gases faster in the cell. This also allows that the RCB bend itself in the middle, decreasing its size and making it easier its passage through smaller blood vessels. (Novais, 2012)

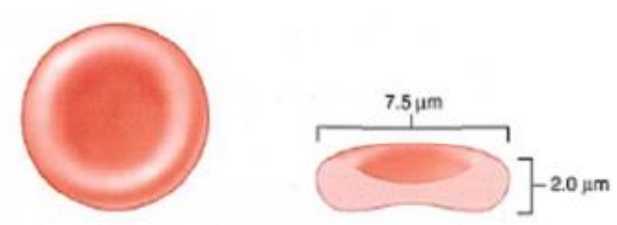

Figure 2 - Shape and size of the RBC.

White blood Cells (WBC)

The white blood cells or leucocytes (

Figure 3) are cells light or whitish without haemoglobin, but with a nucleus. They are bigger than the RBC and equally deformable, but they exist in a smaller quantity. Their principal function is the organism defence WBCs remove dead cells and strange bodys from the organism. The pus is an accumulation of dead WBC and bacterias, togetfher with cellular fragments and liquid. (Novais, 2012)

The WBC can be divided in three groups, the lymphocytes, the monocyte and the granulocytes which can be mononuclear or poly nuclear (neutrophil, Basophil and eosinophil). (Novais, 2012)

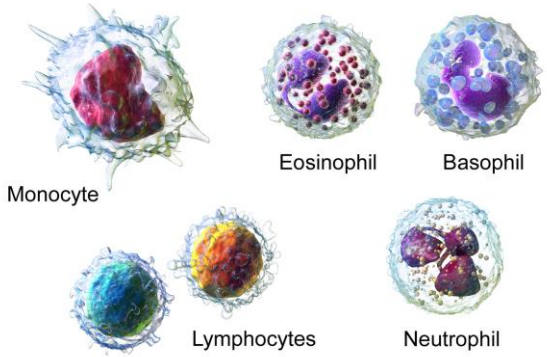

Figure 3 - White blood cells.

Platelets

The platelets are small oval cells that participate in the coagulation process of the blood. Their principal function is allowing the formation of blood clots for the prevention of blood loss if a haemorrhage occurs. The platelets are produced in the bone marrow from megakaryocytes, which are extremely big cells with diameters that can reach 100µm. Their average time in the circulation is about ten days. (Novais, 2012)

Plasma

Plasma is a liquid yellowish and light having numerous substances in solution or suspension that represents about 10% and the rest is water (Novais, 2012).

6. **Hemodynamics in microcirculation**

Human blood is a complex fluid composed mainly of suspended deformable RBCs within plasma. Blood flow behaviour in microcirculation depends on several combined effects such as cell deformability, flow shear rates and geometry of the microvessel, as well as biochemical and biophysical factors which may also affect the rheological characteristics of blood.

A well-known hemodynamic phenomenon, known as Fahraeus-Lindqvist effect, observed in both in vivo and in vitro studies states that for narrow microtubes (<300 µm) both hematrocit and apparent blood viscosity decreases as the tube diameter is reduced (Pires et aI. 1992, Goldsmith et aI. 1989, Novais *et al.* 2014). The physical reason behind

this phenomenon is related to the tendency of the RBCs to undergo axial migration induced by the tank treading motion of its deformable cell membrane as a result of the high shear stresses developed around the wall, and the parabolic velocity profile which forces the RBCs to move towards the centre of the vessel (Caro et aI. 1978. Garcia et aI. 2012. Maeda 1996a. Lima et aI. 2012a, Novais *et al.* 2014), consequently leading to the formation of two phases, i. e., a flow core with mainly RBCs and a cell-free layer (CFL) (Lima et aI. 2009a. Fujiwara et aI. 2009, Lima et aI. 2009b, Novais *et al.* 2014). The CFL formation in microvessels reduces the apparent viscosity of blood and by increasing the CFL thickness the blood viscosity decreases in both microchannels and microvessel, Figure 4. Hence, it is extremely important to understand the behaviour of the CFL in microcirculation as it contributes to the rheological properties of blood flowing in microvessels, it modulates the nitric oxide scavenging effects by RBCs and it may lead to heterogeneous distribution of blood cells in microvascular networks (Fedosov et aI. 2010. Kim et aI. 2009, Novais *et al.* 2014). The cell-free layer width or thickness can be defined as the distance between the wall of the microchannel and the boundary region of the RBCs core (Novais *et al.* 2014).

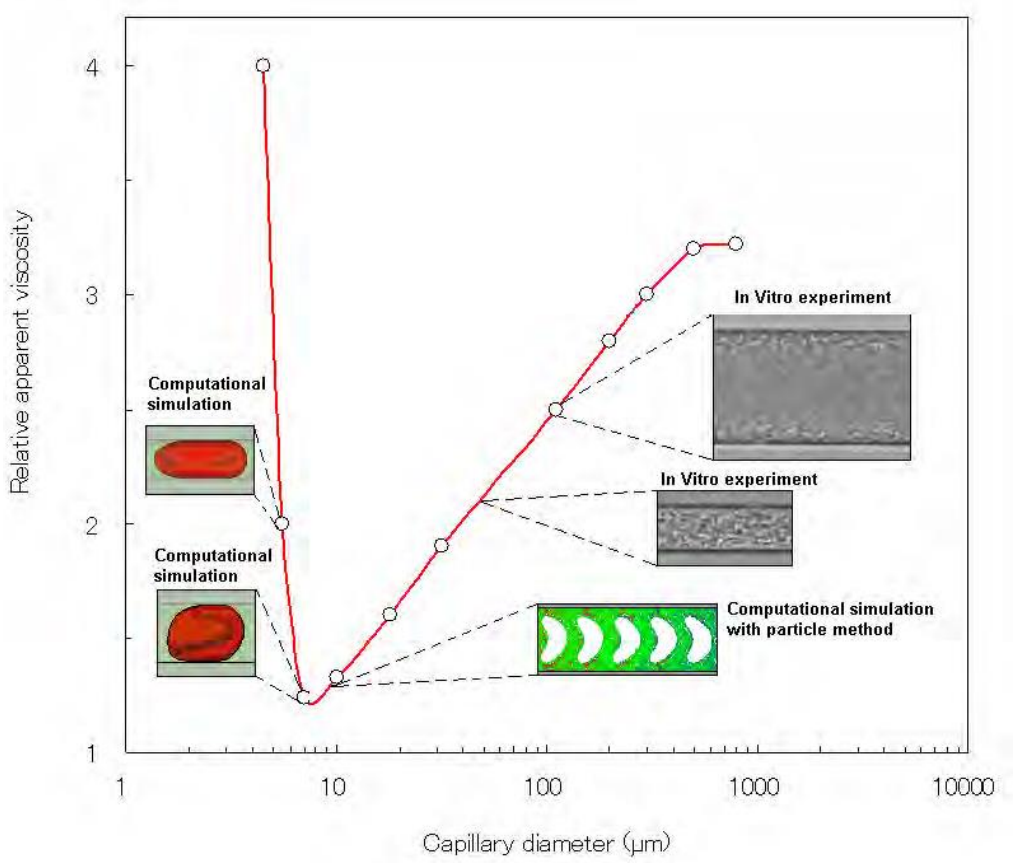

Figure 4 - Relative apparent viscosity of in vitro blood through glass capillaries (adapted from Pries et al., 1992; Wada & Kobayashi, 2002; Tsubota et al., 2006).

Chapter III – Micro fabrication with Lithography

1. Introduction

The lithography is the most used method for microchannels production. Photolithography is a process that transfers a pattern to the *wafer* surface, creating a mould for later being casted with Polydimethylsiloxane (PDMS), see Figure 5.

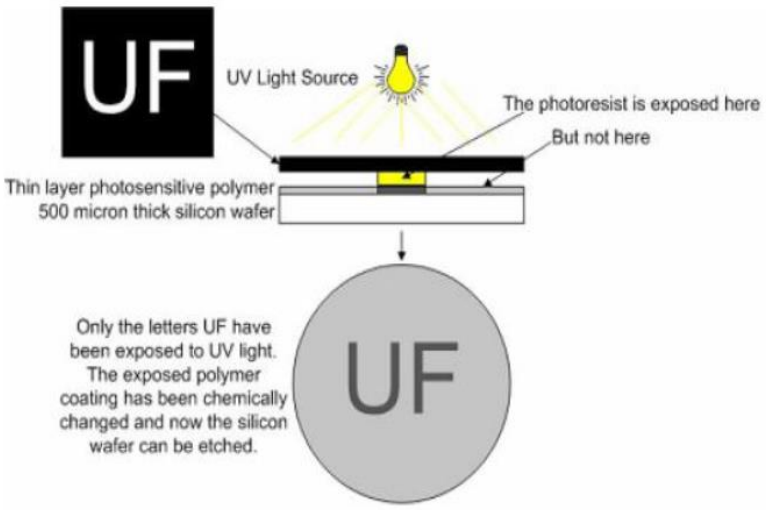

Figure 5 - Photolithography scheme.

This process starts with the creation of a geometry, which is drawn in CAD format. This drawing will then be impressed for the conception of a mask. This mask is normally transparent and done in quartz or soda lime, in which the design that was generated by computer is deposited in a thin chrome layer. There are two types of mask production; one has rectangular characteristics produced by a process called generation pattern, and the other has circular characteristics produced with an electron beam. They can be qualified in light field or dark field depending on the resin that's going to be used (Figure 6). The masks with dark field have all their area covered in chromium while the patterns are transparent. For the mask with light field the chromium is deposited in the areas that have the pattern, while the rest of the area stays free.

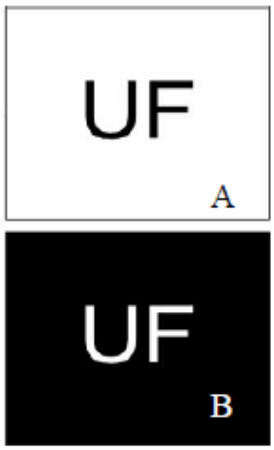

Figure 6 - Example of drawings for masks. A is light field, B is dark field.

The photolithography is a process of microfabrication that has four steps, which are: photoresist application, mask alignment, Ultra violet (UV) radiation exposure, and revelation of the photoresist. For the first step, the photoresist is a polymer that is photosensitive, which allows for the geometry drawing to be transfered into the *wafer*. The thin layer of photoresist is usually applied in the *wafer* by a rotational process, for instance, a spin coater process. There are two types of photoresist, the positive and the negative. The positive becomes soluble when UV radiation is exposed and in turn the drawing areas are dissolved in the development time, and the negative is less soluble, where the areas that are not desirable are dissolved in the development time.

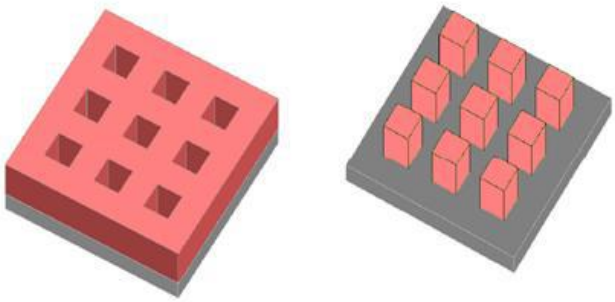

Figure 7 - Schematic representation of the results with the development of the photoresist. Positive photoresist (left) and negative resist (right).

After the *wafer* is covered by the chosen photoresist, the mask is aligned above the *wafer* and the UV light passes through the light parts of the mask to the photoresist on the *wafer*.

The last step is the development of the photoresist, where the *wafer* is placed in the development solution to remove soluble areas.

The *wafer* can be the microchannel if sealed, or the mold for PDMS deposition. PDMS would then acquire the solidified microstructures present in the mold. Subsequently the sealing is done and the channels are ready for fluid flow test (Pinto, 2012).

PDMS is a silicone elastomer and has been the most popular soft material in biomedical microfabrication applications due to very suitable physical and chemical properties, see Table 1 (Makamba, et al. 2003; McDonald and Whitesides, 2002; Toepke and Beebe, 2006, Faustino, 2012). Figure 8 shows PDMS structure.

Table 1- Physical and chemical properties of PDMS (Adapted from McDonald and Whitesides, 2002, Faustino, 2012).

Property	Characteristic	Consequence
Optical	Transparent; UV cut off, 240nm.	Optical detection from 240 to 1100 nm.
Electrical	Insulating: breakdown voltage, 2e7V/m	Allows embedded circuits; Intentional breakdown to open connections.
Mechanical	Elastomeric; tunable Young's modulus, typical value of ~750kPa	Conforms to surfaces; allows actuation by reversible deformation; Facilitates release from moulds.
Thermal	Insulating; thermal conductivity 0.2W/(m.K); coefficient of thermal expansion, 310μm/(m.ºC)	Can be used to insulate heated solutions; does not allow dissipation of resistive heating from electrophoretic separation
Interfacial	Low surface free energy ~20 erg/cm2 contact angle of Sylgard-184: ~110º	Replicas release easily from moulds; can be reversibly sealed to materials
Permeability	Impermeable to liquid water; permeable to gases and nonpolar organic solvents; oxygen diffusion coefficient 3.55×10-5 cm2/s	Contains aqueous solutions in channels; allow gas transport through the bulk material; incompatible with many organic solvents
Reactivity	Inert; can be oxidized by exposure to a plasma; Bu4N+F-((TBA)F)	Unreactive toward most reagents; surface can be etched; can be modified to be hydrophilic and also reactive toward silanes; etching with (TBA)F can alter topography of surfaces
Toxicity	Nontoxic	can be implanted *in vivo*; supports mammalian cell growth

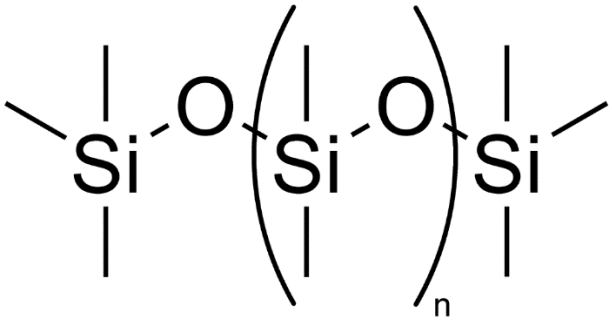

Figure 8 - PDMS structure.

7. **Methodology**

In this work we started with a wafer already ready as a mould, which was created with a negative photoresist SU-8. The soft lithography process begins with the casting process. This process uses the PDMS for creating the microchannel.

7.1. Casting process

Figure 9 - Materials for the PDMS production.

We started with producing two different mix ratios of PDMS and Curing agent, 10:1 (for channel substrate) and 20:1 (for sealing the channels). Figure 9 shows materials for PDMS production. After the mixing of PDMS and curing agent, the mixture needs to have the bubbles removed with a vacuum pump (Figure 10). To remove the bubbles faster the air was allowed to flow in the vacuum chamber for brief periods of time.

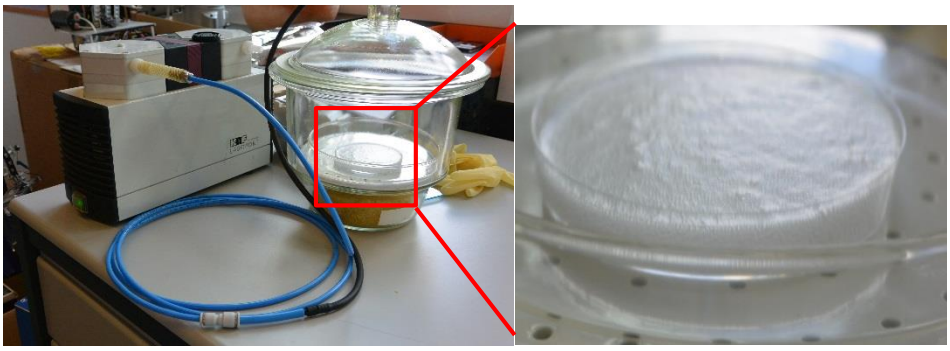

Figure 10 - PDMS inside the vacuum pump to remove the bubbles.

After the bubbles removal, the PDMS with the ratio of 10:1 was carefully dispensed over the mould and degased again, since some bubbles are created again from the process of pouring (Figure 11).

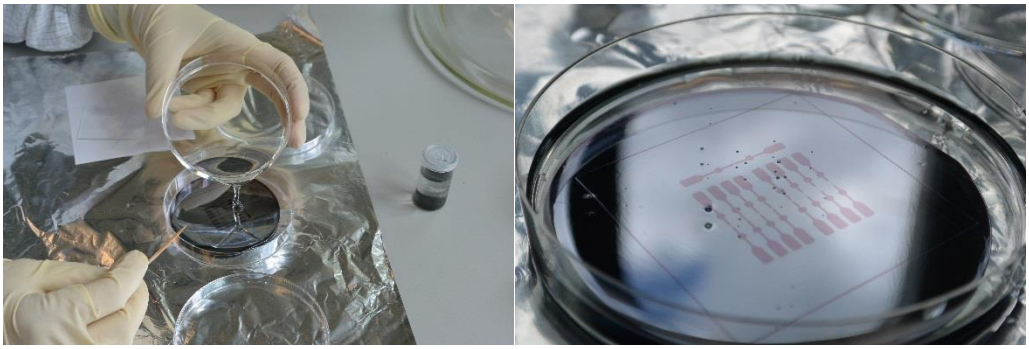

Figure 11 - The left shows the dispense of the PDMS over the SU 8 mould, and the right shows some bubles formed after the dispense.

The next step is to put the PDMS in the oven at 80°C for about 20 minutes. During this process, we create the PDMS with ratio of 20:1 for the sealing glass. Using the Spin coater we coat a thin glass with the PDMS mixture and put this glass also in the oven at 80°C for about 20 minutes.

After cooling down the microchannel, we cut the channel (PDMS substrate) and make the holes for the inlet and outlet with the help of a precision tip. It is important to make sure to remove the residues from the punching process. To avoid impurities the channels shouldn't be touched, however if it happens use brown adhesive tape to clean it. Finally we place the PDMS side of the glass in contact with the open channel side of the PDMS substrate, and bake for further 12 to 24 hours at 80ºC (Figure 12).

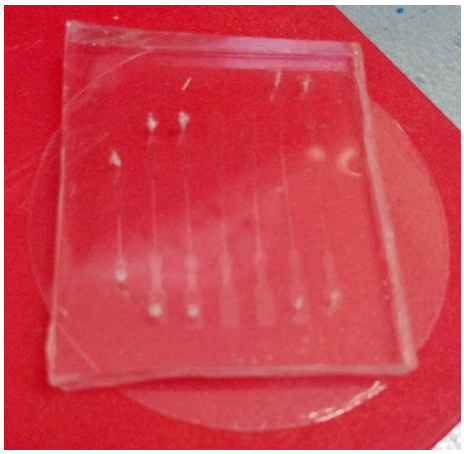

Figure 12 - Microchannels produced by soft lithography.

8. **Results and Discussion**

The drawings for the mask used to the wafer in SU 8 are presented in Figure 13 and Figure 14.

8.1. Hyperbolic microchannels

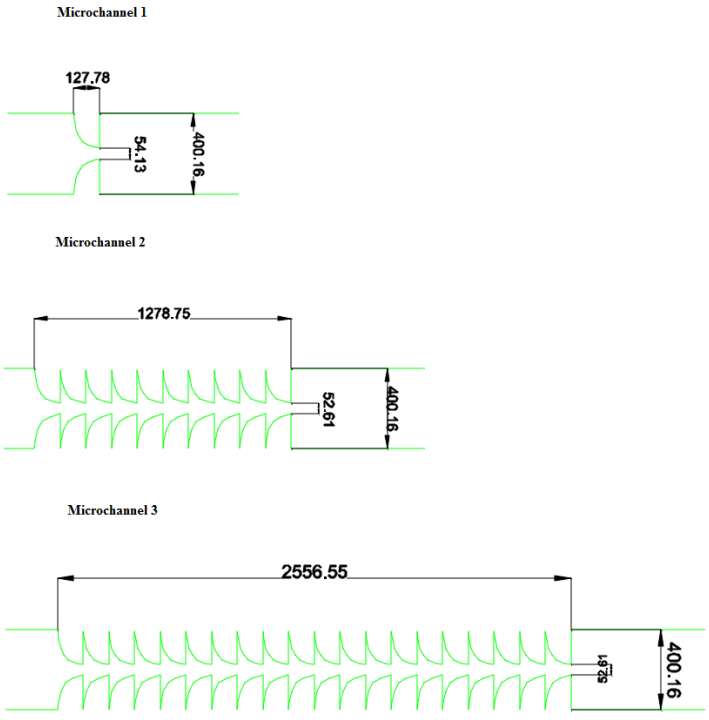

Figure 13 - Hyperbolic channels 1, 2 and 3 (µm).

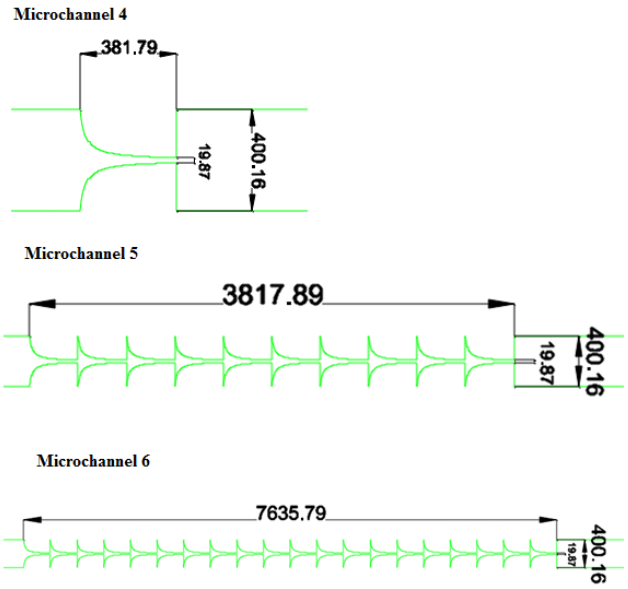

Figure 14 - Hyperbolic channels 4, 5 and 6 (µm).

8.2. Blood flow visualization

The setup used for the blood flow visualization is shown in Figure 29Figure 29 The blood used was from ovine and the hematocrit was set to be 5%.

For the measurement of the CFL, the starting measurement point was set to be 150 µm downstream the exit of hyperbolic contraction region where the CFL thickness reach steadiness (see Figure 15).

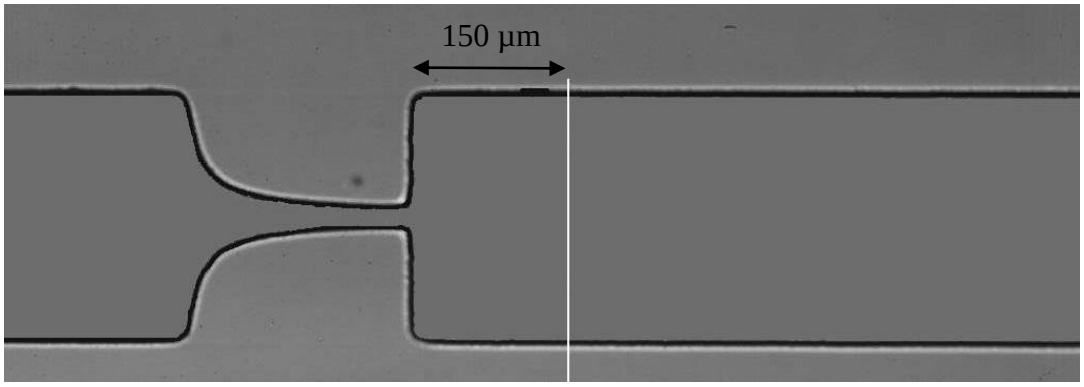

Figure 15 - CFL measurement starting point in grey line.

8.3. Channel 1, 2 and 3

For channel 1, 2 and 3 it is possible to see that before and after the hyperbolic contraction there is no CFL as presented in Figure 16. This qualitative results show that even by increasing the number of hyperbolics we do not have a CFL after the contractions.

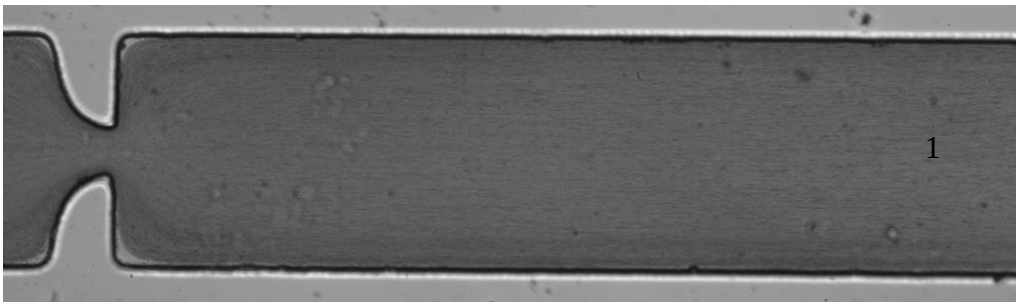

20x objective

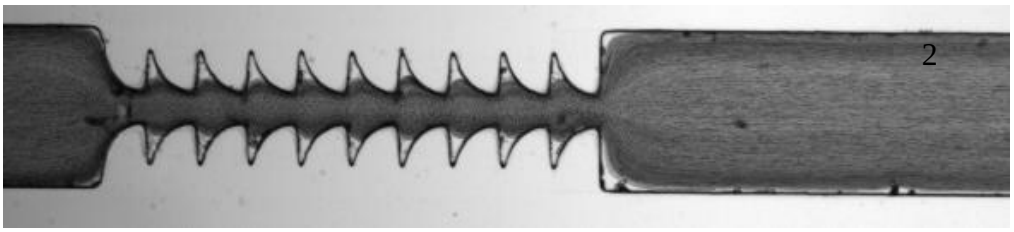

10x objective

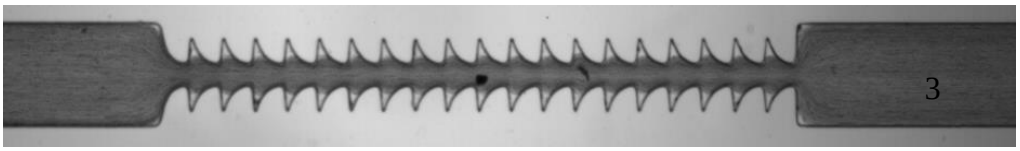

4x objective

Figure 16 - Blood flow images obtained from Image J (Zproject plugin) of channels 1, 2 and 3 with a flow of 10 µL/min.

8.4. Channel 4, 5 and 6

For channel 4, 5 and 6 it is possible to see that before the contraction there's no CFL (Figure 17), however after the hyperbolic contraction there's CFL as presented in Figure 18. Table 2 summarises the CFL thickness measured for these microchannels, downstream the contraction.

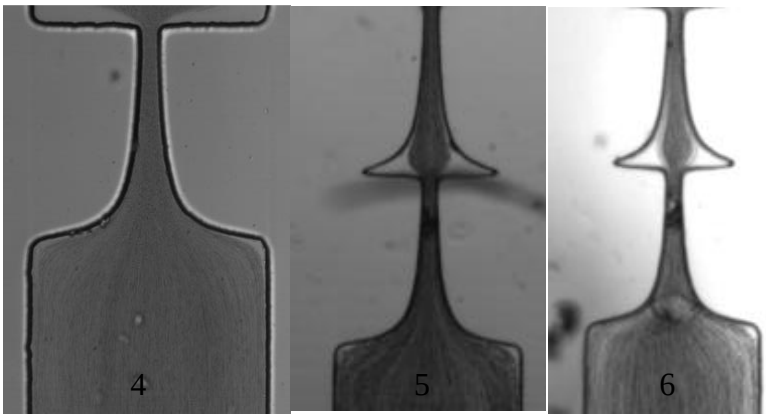

10x objective 10x objective 10x objective

Figure 17 – Blood flow images obtained from Image J (Zproject plugin) for the entrances of channel 4, 5 and 6 with a flow of 10 µL/min.

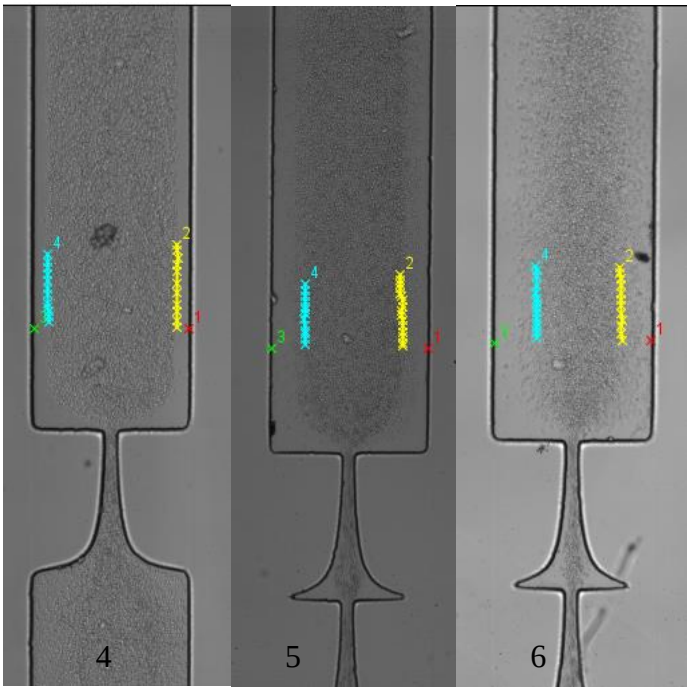

Figure 18 - Tracking blood cells (MtrackJ plugin from ImageJ) around the cell free layer: The tracking results were used to determine the plasma thickness.

Table 2 - CFL thickness in µm.

	Channel		
	4	5	6
Left	34,84	83,49	103,15
Right	30,10	65,68	75,33

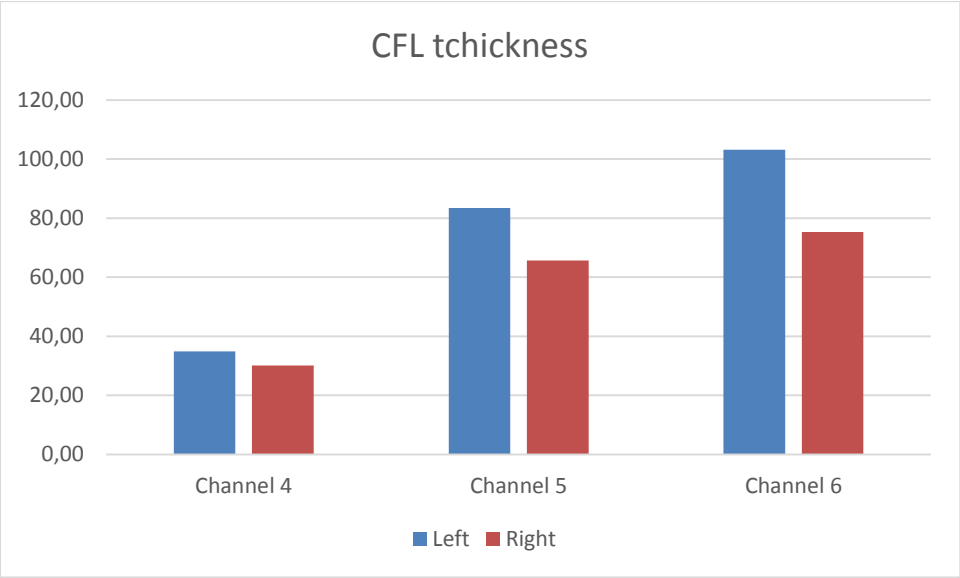

Figure 19 - Graphic of CFL thickness in µm .

In channels 1. 2 and 3 there was no CFL presence mainly because of the hyperbolic contraction width (~52 µm). In channels 4, 5 and 6 where the contraction width was smaller (20 µm) CFL was formed. Additionally, the results show that the CFL thickness increases by increasing the number of hyperbolic contractions as shown in Figure 19. This latter microchannel may promote high levels of flow recirculations around the hyperbolics corners and this phenomenon may be the main reason to increase the CFL thickness. Future work is needed to confirm such phenomenon.

Chapter IV – Micro fabrication with a milling machine

1. Introduction

The micro milling is the process of milling in a micro size that is usually used in the creation of PCB boards. This consist in a mechanical method, which use a small revolving tool to produce the polymer microstructures removing the material. The movement and position of the tool are controled by the computer, which is a serial process known by computer numerical control or CNC. Like laser machining, CNC milling is a serial process. The milling process tends to be slower than laser machining, since the cutting tools can break easily because they are really fragile (Geschke, et al, 2008). The smaller the tools are the more fragile they are. There is the possibility of going smaller than 30 µm, which is the smallest size in this work, since there are new tools being created, of which size is 20µm tool, however that requires some precautions for not breaking the tool, cf. Figure 20.

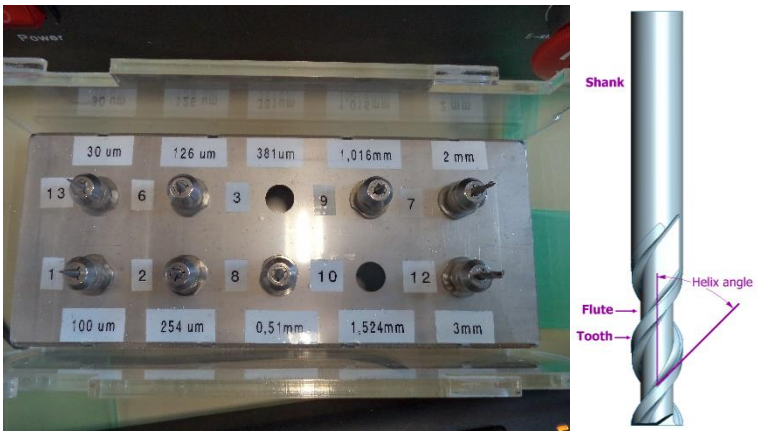

Figure 20 - Milling Tools and a sketch of a milling cutter.

This process has the advantage of not chemically degraded the polymer by heating or UV radiation, like laser micro milling (Figure 21). However it is possible to leave some stress and tension near the cut grove or cavity, which can be relieved by the use of a cooler like water or air. Micro milling can only be used with hard materials, like thermoplastics, PMMA and COC, as long as the milling does not heat the material too much. Elastomers usually cannot be milled (Geschke, et al, 2008).

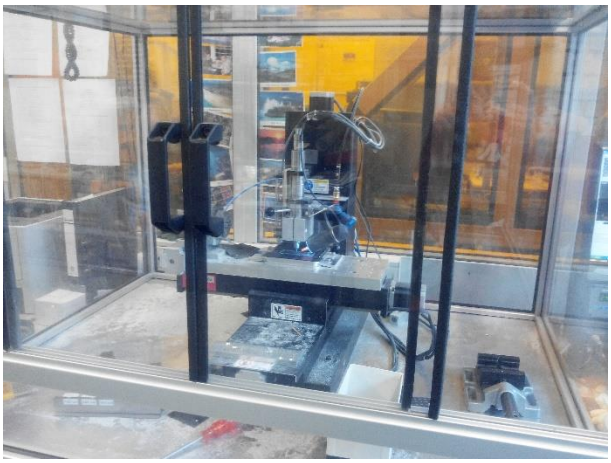

Figure 21 - Micro milling machine (Minitech Mini-Mill/GX).

The material milled in this project was PMMA (polymethyl methacrylate), also known by acrylic glass or Plexiglass®. This material is a clear plastic acrylic which can replace glass, which usage goes to hockey rinks, signs and lenses. It's a rigid thermoplastic, transparent and colourless.

It is a material produced by emulsion polymerization, solution polymerization and bulk polymerization, where it is necessary to have a ratio from 2 kg of petroleum for 1 kg of PMMA.

This material is often compared to glass, as shown in the Table 3 - Glass vs PMMA Table 3 (Webopedia, MicroChem, Wikipédia, SetorVidreiro). Figure 22 shows the PMMA structure.

Table 3 - Glass vs PMMA

	Glass (SLSG)	**PMMA**
Melting Point	600ºC	160ºC
Density	2500 Kg/m^3	1180 Kg/m^3

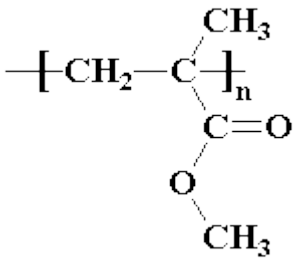

Figure 22 - PMMA structure.

9. **Methodology**

The process for the construction of the microchannels passes through three softwares, namely AutoCAD, Visual Mill and Minitech.

With the first software AutoCAD, the microchannel geometries are drawn. The next step is programming the milling process, which is done in Visual Mill, for posting the code in ".nc" to be compatible with Minitech where the actual milling happens. Then the tubes must be made, using a syringe needle of 1.2 ×50 mm which creates 3-4 tubes. Finally all the parts are assembledby a glue. Then the channels are washed in the ultrasonic machine withnormal clean water, blown to dry and sealed with an adhesive film.

9.1. AutoCAD

The first step is the drawingby using AutoCAD. In every drawing there are some aspects to be considered, having an example in Figure 23:

1. Start the drawing in the position (0,0) or move it in the end;
2. The scale used for this milling machine is 1unit=1mm, but the scale can be changed after the drawing;
3. Must consider the mill tool size to the drawing. For example, for a 100 μm drawing you use the 100 tool, or smaller;
4. Close all the polygons. The milling is done by parts, each of which has its polygon;
5. For the entrances and exits two circles or similar must be created, with an outside circle with 2mm and the small with 1.24 mm of diameter;
6. Save it in ".dxf" format.

Figure 23 - Example of a microchannel prepared for the milling process, all polygons are closed.

Use a program like “LinkCad” to be sure the polygons are closed.

9.2. Visual Mill

This software is used to create the movements of the milling machine. Here we define the depth, velocity, angle, etc. (Figure 24). Like AutoCAD it is necessary to consider some things. Because the table is not in the same level, some parts are higher than others. In the same way, different milling tools have different heights and small tools are really fragile (small tool is considered to be 100µm or less,). Because of the usage of different tools for the same channel, some precautions have to be taken, in order to have better results:

1. Start with the middle size tool. For each channel you must do a program;
2. Change to the smaller tool, if necessary. The configuration must be done for each channel;
3. Finally do the holes for the tubes. One configuration is enough.
4. Save and post each configuration. Close “Visual Mill”, so it does not interfere with the next program.

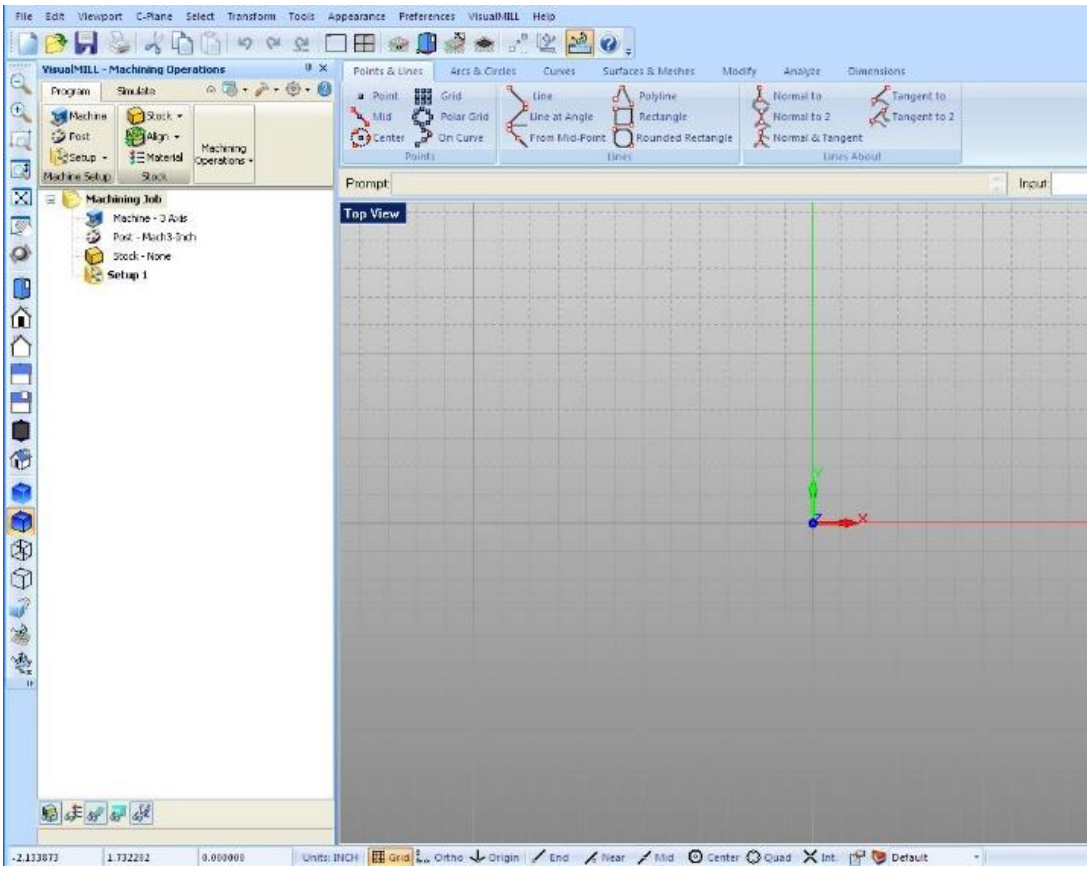

Figure 24 - Visual Mill desktop.

9.3. Mini Tech

The set-up used for the milling process is shown in Figure 25. It is composed by two computers, one of which is connected to a microscope turned to the tool for observation; and the other have Minitech software. In the middle there is the micro milling machine.

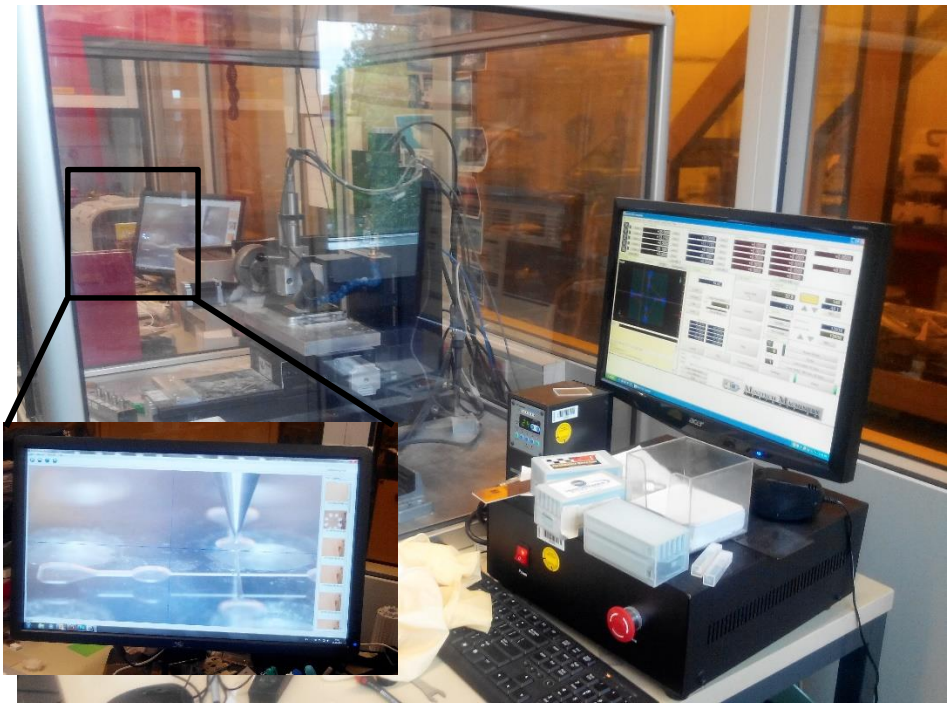

Figure 25 - Setup of milling process. (From back to the front) Screen of the image of the microscope pointing to the tool, the Milling machine and finally the computer with the software for milling.

Minitech reads the code and transformed it in the milling process. The special attention has to be made for the zeros, especially in the z axis, since this decides if the channel stays always with the same depth. So for z=0 you have to position the tool close to the channel place, and slowly lower the rotating tool. When the point of the tool is really close to the PMMA glass, you must change for small steps of 0.005 µm or smaller and stop when the first touch is done, and this is to be the zero position (Figure 26).

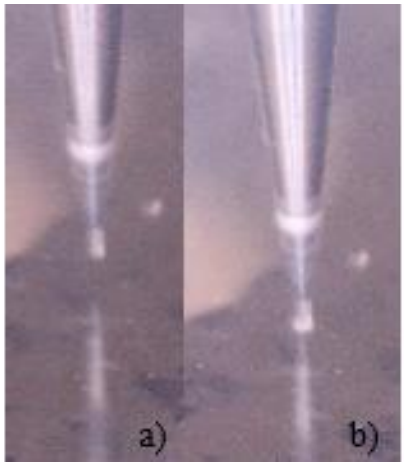

Figure 26 – a) The tool really close to the PMMA, while the b) The first touch.

This process is done for every part of the channel with the exception of the in/outlets, where the zero is calculated in the middle of the Plexiglass.

When the milling is finished, the acrylic glass should be washed with water and soap with circular motions and blown with oxygen for drying. In this part the deep measurement should be done.

9.4. Tubes Production, assemble and cleaning

This process consists in the cutting of the syringe needle in small parts of about 1 cm of length, and sanding the tips on both sides. For each in/outlet one, a tube must be produced. Before assembling the tubes with the PMMA, a syringe should pass through the holes for an easy insertion of the tubes. The tubes should be inserted from the top to the entrance/exit of the channel.

After assembling, as shown in Figure 27, we use a resin and its hardener mixed with a ratio of 1:1. The mixture is put a little bit in each tube, near the Plexiglass. Once it got dry, the channel should go to the ultrasonic machine to be washed for about 10-15 minutes at 100ºC, in a mix of water with glass washer.

Finally, the channels are blown with nitrogen to dry the device and sealed with the adhesive film, using some strength.

Figure 27 – a) Setup for tubes production, with an assembled channel. b) Resin and Hardener used to glue the tubes to the Plexiglass. c) Final product.

9.5. Testing

Some images were acquired with the microscope Sensofar, with it is possible to have a perspective of the actual height of the channels (Figure 28).

Figure 28- 3D optical profiler (Sensofar, plu neox).

The setup used to do the experiments was the shown in Figure 29. It is composed by the computer, the syringe pump (Harvard Apparatus PHD ULTRA), the high speed camera (FASTCAM SA3, Photron) and the inverted microscope (IX71, Olympus).

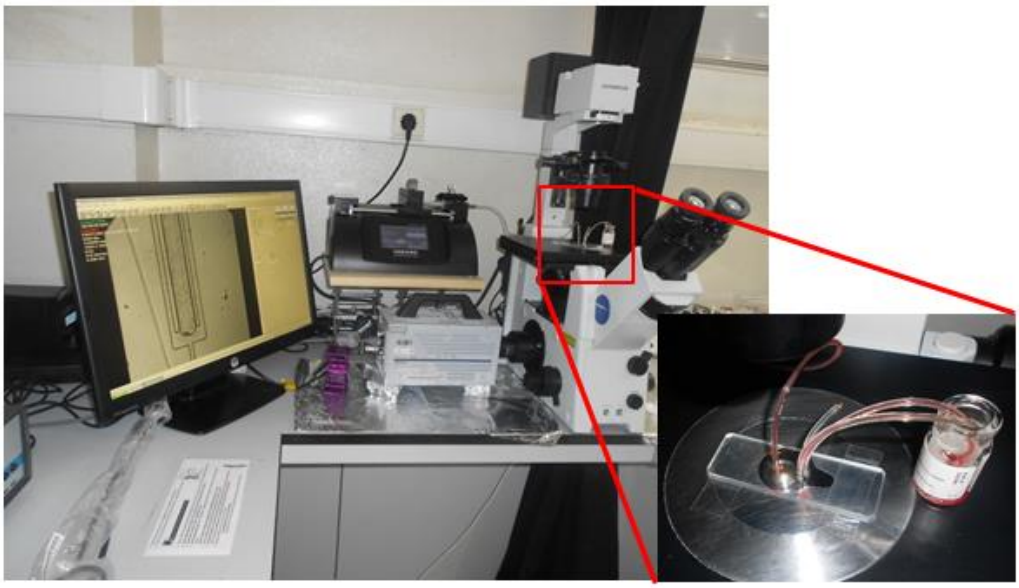

Figure 29 - Setup for the CFL measurement.

10. Results and Discussion

As it was explained in the methodology, the drawings of the microchannels were first made in the AutoCAD.

10.1. Simple contraction microchannels

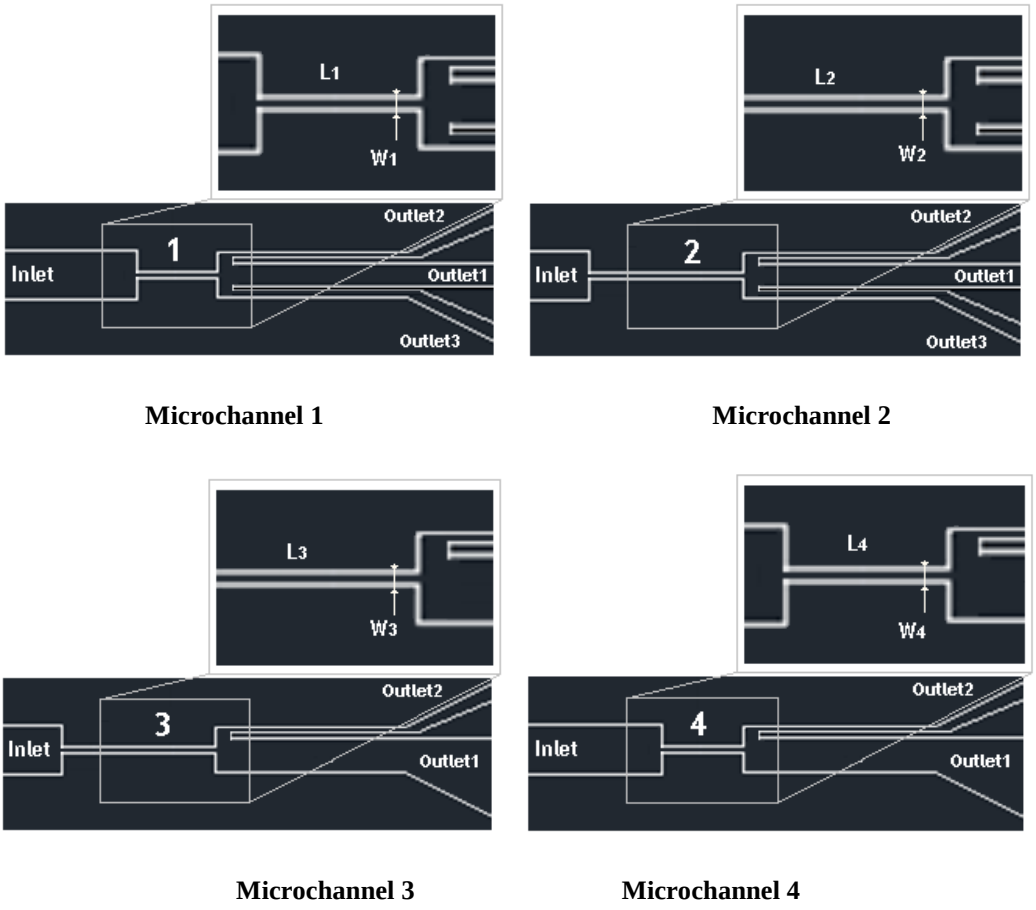

Microchannel 1 **Microchannel 2**

Microchannel 3 **Microchannel 4**

Figure 30 – Simple contraction microchannels: W (inlet width) = 300 µm, L_1=520 µm; W_1=30 µm; L_2=2000 µm; W_2=30 µm L_3=2000 µm; W_3=30 µm L_4=520 µm; W_4=30 µm

As Figure 30 shows, the microchannels with simple contractions were the first to be made, being made by two different fabrication strategies. For example, for the first strategy, downstream of the contration, the machinable microchannels did not have an uniform height and the walls of the separation part did not have the same width. As a result, we have decided to improve the fabrication methodology to try to minimize such kind of irregularaties (strategy 2).

There are two different types of microchannels: simple contraction microchannel with three outlets (1 and 2) and simple contraction microchannel with two outlets (3 and

4). For each type the length (L) of the contraction is different. Note that the center outlet is intended to have mostly RBCs and the other outlets mainly plasma.

Measurement analysis

To evaluate both fabrication strategies the depth of microchannels were measured by using the Sensofar microscope. The results obtained by this microscope are presented in Figure 31 and 32, where a) represents the first strategy and b) the second one. Note that, the second strategy was improved due to the experience acquire from the first strategy.

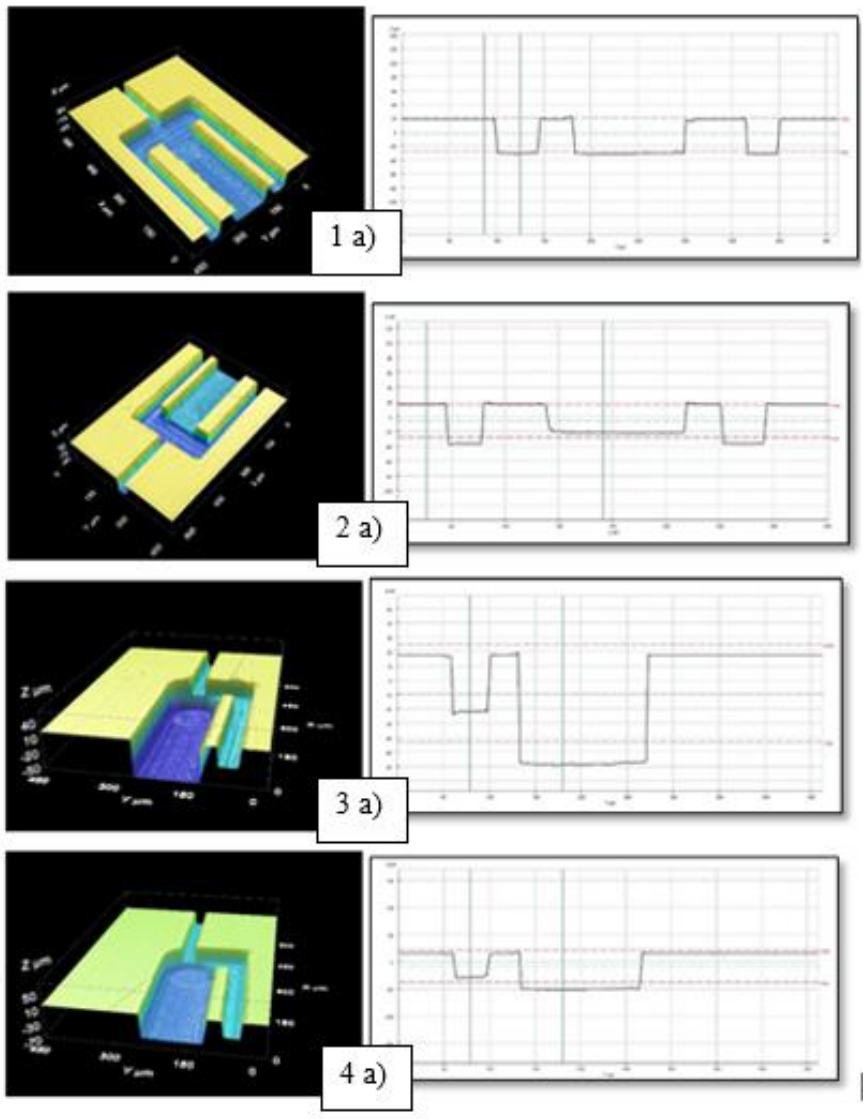

Figure 31 - Measurements of the microchannels performed by the first strategy. All measurements were obtained by a Sensofar microscope.

In the figure above it is possible to visualize that in the microchannels 2a), 3a) and 4a) the depth along the microchannel is not uniform. For the microchannel 1a), although the depth is uniform the walls at the separation part (downstream the contraction) have

different widths. This fabrication problem also happens in the microchannel 2b). For the next strategy, in order to obtain a more uniform depth and wall thickness, the precautions spoken in the methodology were taken in to account.

Figure 32 shows the microchannels geometries performed by the second strategy. It is possible to visualize that the depths are more uniforms, however the difference between the walls thickness remains not so precise, and as a result future work is needed to improve this region of the microchannel.

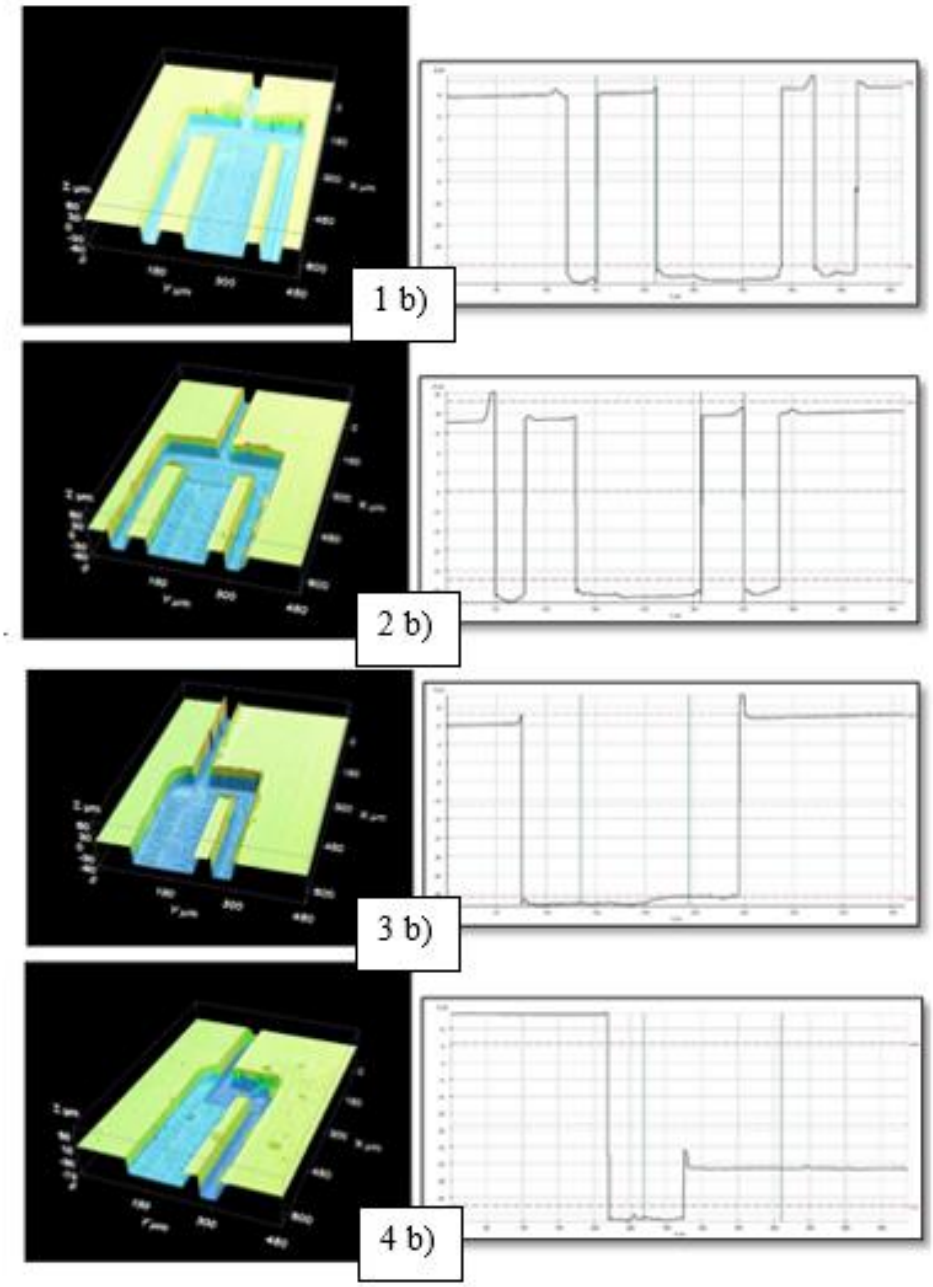

Figure 32 - Measurements of the microchannels performed by the second strategy.

The Table 4 shows the differences between the two strategies. By using Sensofar microscope it was possible to calculate the depth differences at the regions downstream

the contraction. Generally, the results from Table 4 show that the second strategy generates microchannels with much better uniform depths.

Table 4 - Difference in the depths at the regions downstream the contraction, in µm.

	Channel			
	1	2	3	4
First strategy (a)	> 1	15,406	36,329	22,515
Second strategy (b)	1,1209	1,9263	2,0143	14,22

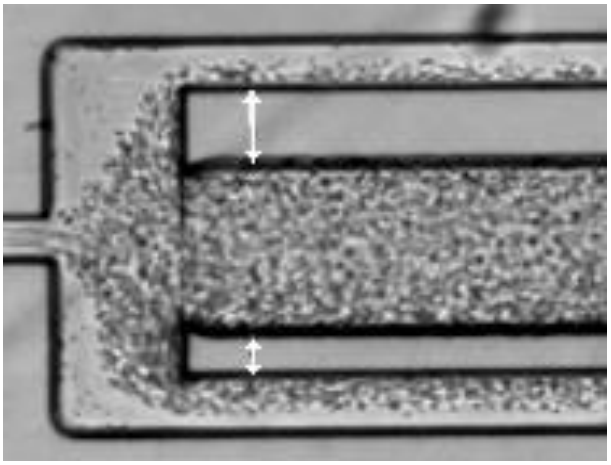

Figure 33 - Example of the wall thickness difference at the regions downstream the contraction.

To determine the divergence of the walls of channel 1 a), 1b), 2a) and 2b) some calculations were made, with ImageJ. Table 5 shows the thickness of the walls at the left and right side and its difference. This fabrication imperfection may influence the results of the blood flow.

Table 5 - Thickness of the side walls calculated by ImageJ (µm).

	Channel			
	1a)	1b)	2a)	2b)
Left	51,977	41,534	48,588	53,417
Right	28,249	34,756	23,729	26,285
Diference	23,728	6,778	24,859	27,132

10.2. Blood flow visualization

Figure 34 shows examples of the microfluidic devices used to perform blood flow visualization. We have tested a total of 8 different microchannels using two different kinds of strategies.

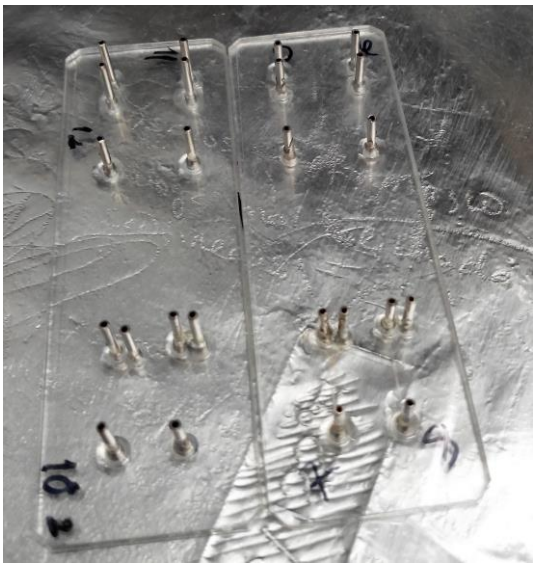

Figure 34 - Microfluidic devices used to perform blood flow visualization.

The tests were made with different flow rates and hematocrits, however in this study we will show mainly the results with a flow rate of 5 µL/min and a hematocrit of 5 %.

Microchannel 1

Figure 35 shows the flow of blood cells in the microchannel 1 for both strategies a) and b). From these qualitative images, obtained from Image J (Zproject plugin), it is clear that the contraction increases the cell free layer (CFL) and consequently may improve the separation efficiency. This phenomenon happens for both fabrication strategies.

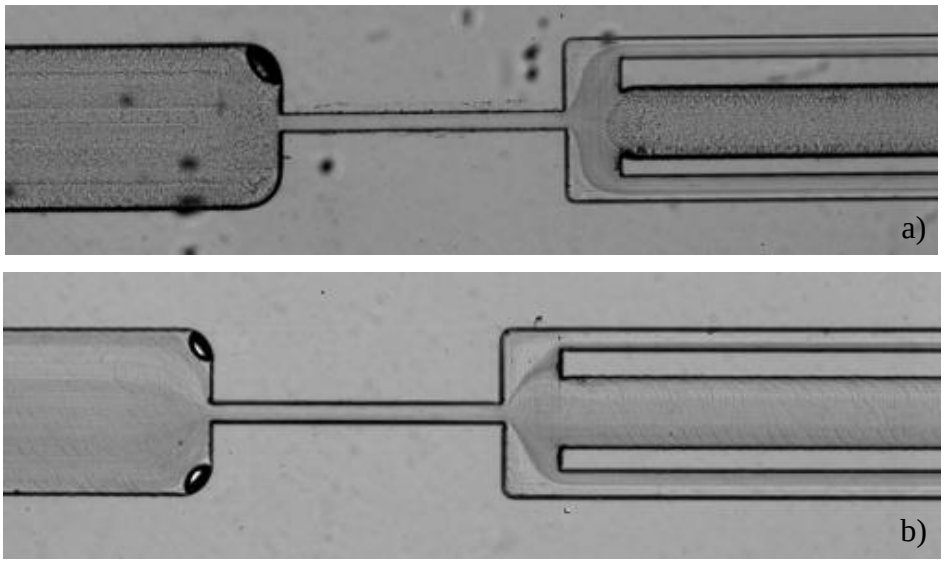

Figure 35 - Blood flow images obtained from Image J (Zproject plugin): a) microchannel from the first strategy; b) microchannel from the second strategy.

Figure 36 shows the tracking of blood cells performed by the MtrackJ plugin from ImageJ. By tracking individual red blood cells around the CFL it was possible to determine the CFL thickness.

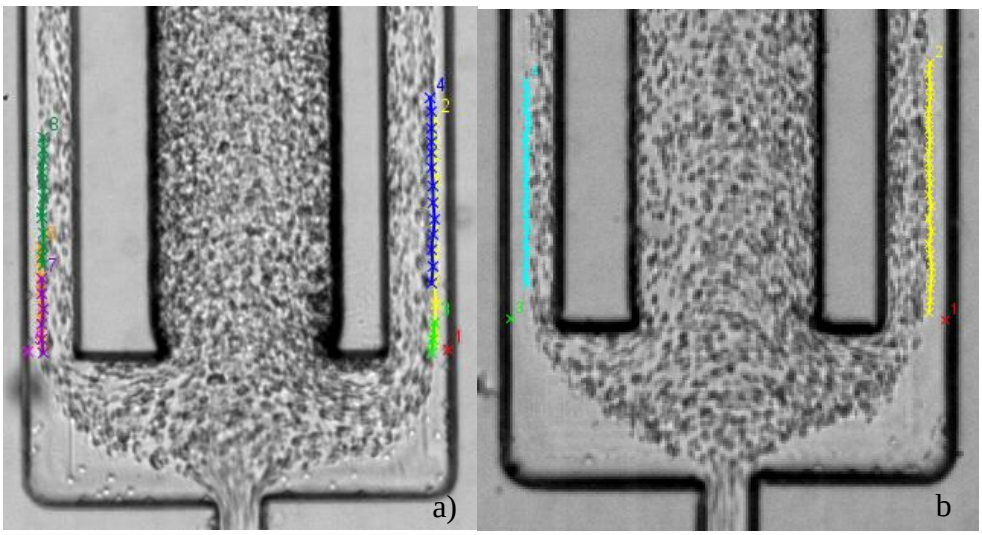

Figure 36 – Tracking blood cells (MtrackJ plugin from ImageJ) around the cell free layer: a) microchannel from the first strategy; b) microchannel from the second strategy. The tracking results were used to determine the plasma thickness.

Microchannel 2

Figure 37 shows the flow of blood cells in the microchannel 2 for both strategies a) and b). The qualitative results show once again that the contraction increases the CFL and happens for both fabrication strategies.

a)

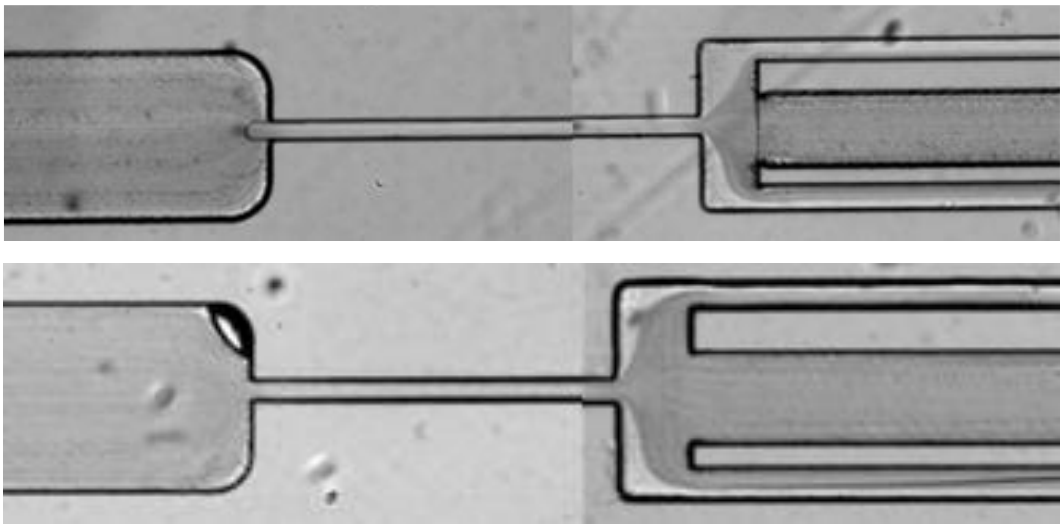

Figure 37 - Blood flow images obtained from Image J (Zproject plugin): a) microchannel from the first strategy; b) microchannel from the second strategy.

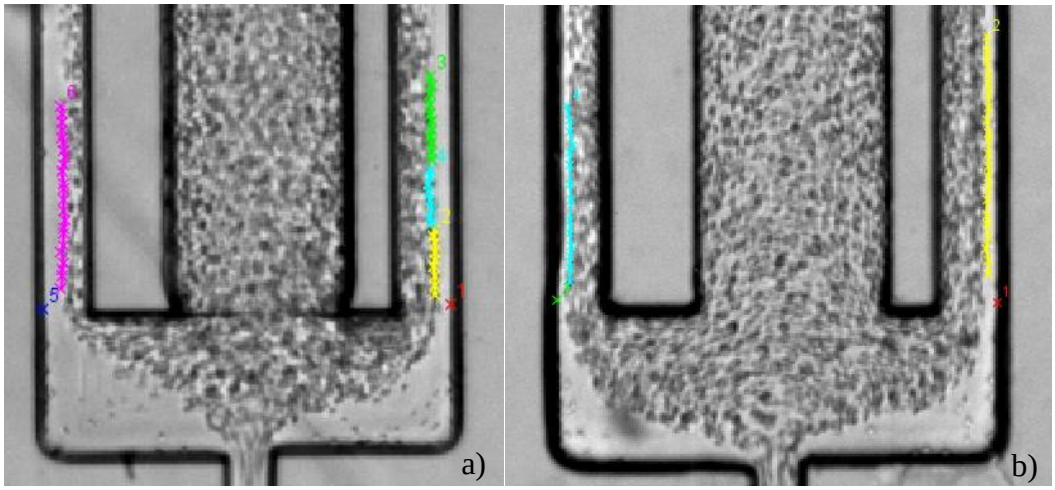

Figure 38 - Tracking blood cells (MtrackJ plugin from ImageJ) around the cell free layer: a) microchannel from the first strategy; b) microchannel from the second strategy. The tracking results were used to determine the plasma thickness.

Microchannel 3

Figure 39 shows the microchannels 3 fabricated by both strategies. Unfortunately both microchannels had fabrication problems and consequently the results obtained by these microchannels were inconclusive.

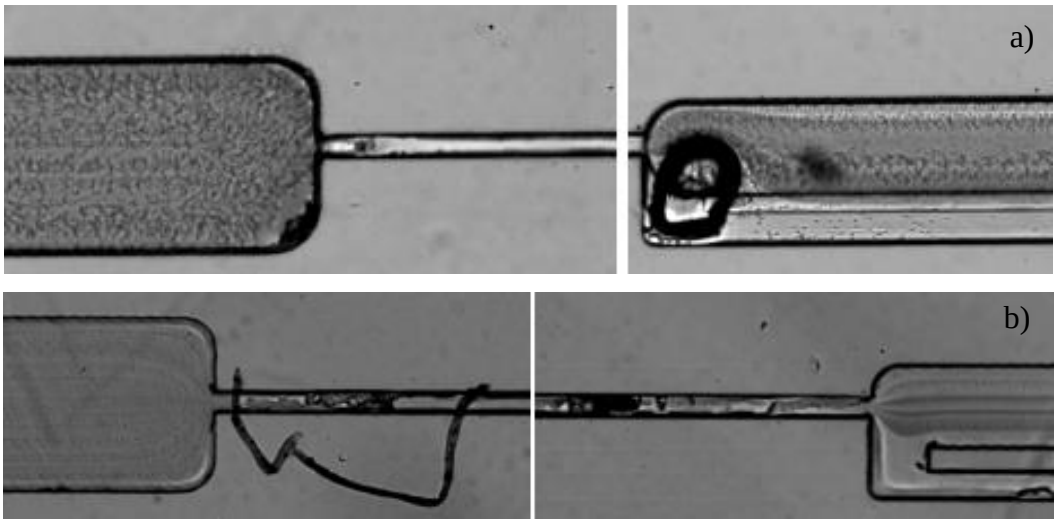

Figure 39 - Blood flow in: a) microchannel from the first strategy; b) microchannel from the second strategy.

Microchannel 4

Figure 40 shows the flow of blood cells in the microchannel 4 for both strategies a) and b). From the qualitative images it is clear that this contraction also increases the CFL and consequently may improve the separation efficiency. This phenomenon happens for both fabrication strategies. Note that for the microchannel 4a) part of the separation width was broken during the fabrication of the device. This unexpected geometry may affect the separation efficiency as is possible to visualize in Figure 40a).

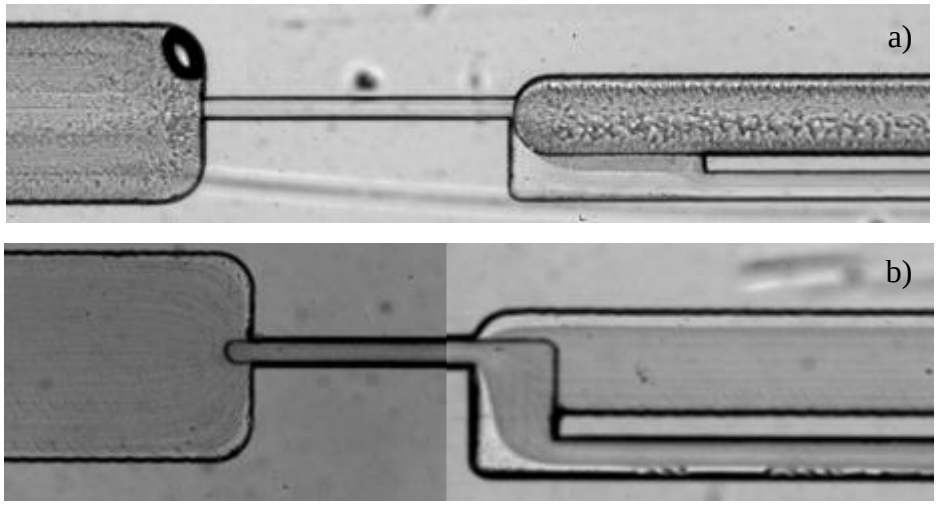

Figure 40 - Blood flow images obtained from Image J (Zproject plugin): a) microchannel from the first strategy; b) microchannel from the second strategy.

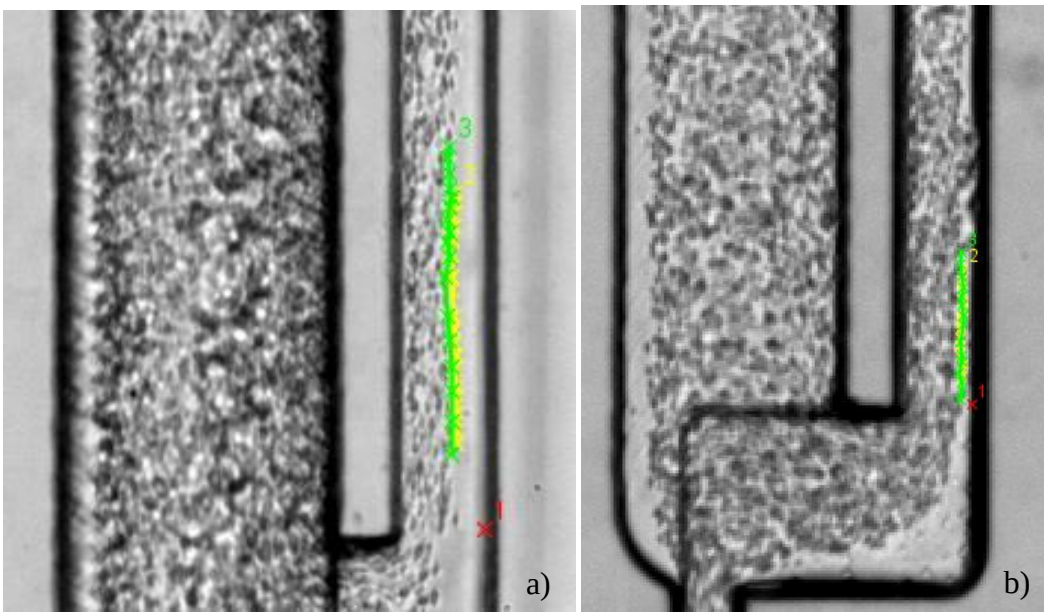

Figure 41 - Tracking blood cells (MtrackJ plugin from ImageJ) around the cell free layer: a) microchannel from the first strategy; b) microchannel from the second strategy. The tracking results were used to determine the plasma thickness.

Figure 41 shows the tracking (MtrackJ plugin from ImageJ) of blood cells performed at a flow rate of 5µL/min. By tracking individual red blood cells around the CFL it was possible to determine the CFL thickness for both microchannels.

The CFL thickness measured from all the microchannels are presented in Table 6. The best result was channel 4a) as the CFL thickness was largest, followed by channel 1a), 1b) and 2a).

Table 6 – CFL thickness comparison from a first stage, in µm.

	Channel							
	1		2		3		4	
Side	a)	b)	a)	b)	a)	b)	a)	b)
Left	9,567	11,042	13,436	8,959	Fabrication problem	Contration dirty and exit closed	-/-	-/-
Right	10,461	10,341	14,024	6,290			15,692	5,750

The CFL thickness for the microchannel 1a) and b) was similar as the only difference was the widths of the separation walls that were not equal. For the case of microchannel 2, downstream the contraction, the depth of the microchannel 2a) around the corners were smaller when compared with microchannel 2b). Hence this lower depth

may have promoted bigger recirculations or vortex around the corners and consequently may improve the cell separation efficiency by increasing the CFL thickness. Similar results happen in the microchannel 4 where the decrease of the depth (microchannel 4a) seems to promote an increase in CFL thickness. Future work is needed to confirm such phenomenon. Note that, for the case of microchannel 3 it was not possible to obtain the CFL thickness due to fabrication problems.

Additionally, for the microchannel 4a) we have also investigated the effect of the flow rate (see Table 7 and Figure 42). The results show that the CFL thickness tend to increase until the flow rate of 25 µL/min, however after that it tends to level off.

Table 7 - Channel 4a) CFL for different flow rates.

Velocity	**5**	**15**	**25**	**35**	**45**	**60**	**80**	**µL/min**
Average thickness	15,69	20,18	24,20	25,18	22,21	24,36	22,37	µm

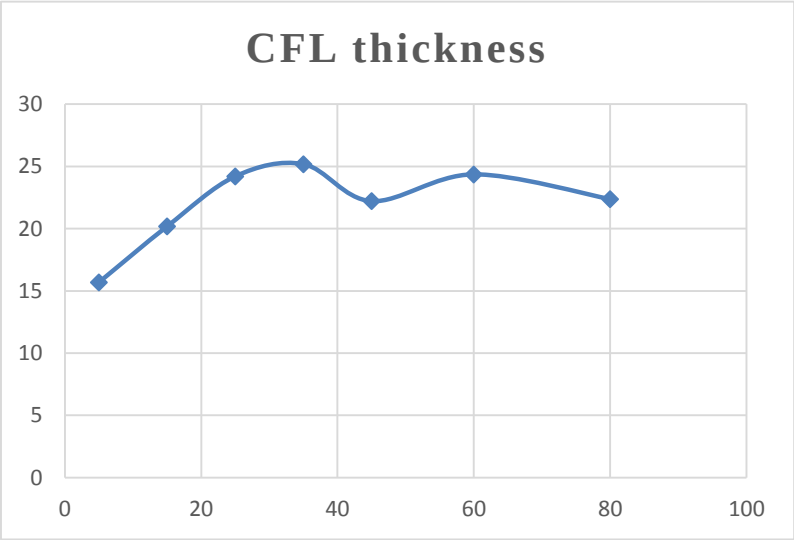

Figure 42 - Microchannel 4a) CFL for different flow rates.

10.3. Other Channels produced

The Figure 43 represents additional microchannels with different types of geometries such as microchannels with hyperbolic contractions, however because some

channels were danified, we have decided not to perform blood flow studies.

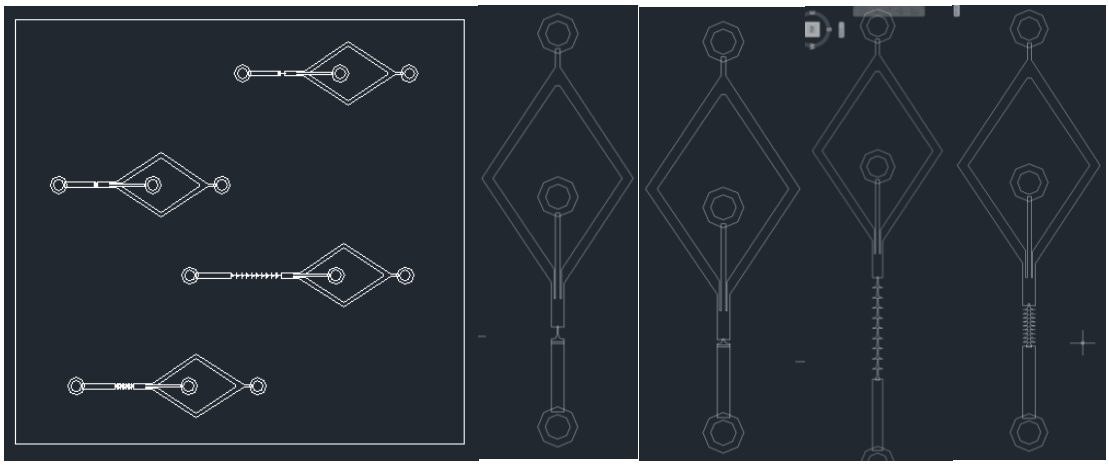

Figure 43 - Hyperbolic microchannels drawings

Chapter V - Conclusions and Recommendations

The purpose of this project was to develop a microchannel and test its efficacy in the separation of cells from plasma. To achieve the aim of the work it was used two types of fabrication, soft lithography and micromilling (low cost approach), and different channel designs.

In the case of the lithography process, it is an expensive, time consuming process, needs a clean room facility and disposable one, i.e., the PDMS microchannels can only be used once. The CFL obtained was not totally free of cells, and to achieve total separation might be harder, nevertheless the cell free layer thickness was relatively high. In this study, we have tested hyperbolic contractions and the results indicate that the microchannel with the smallest contraction width (20 μm), the CFL thickness tend to increase with the number of hyperbolic contractions.In the micromilling fabrication, the process is cheaper, does not need a clean room and the devices are reusable. The CFL thickness measurements presented good results, particularly for channel 4a). However the fabrication process should be improved since some mistakes occur for the lack of knowledge in the micromilling parameters, for example the thickness difference in the outlet walls or for human error for the depth of the microchannel. Furthermore, new tools should be acquired in a smaller size, since the smaller tool of 30 μm provided good results.

Overall, except for the hyperbolic microchannels with the highest contraction width (52μm), all the other microcontractions where able to increase the CFL downstream the contraction. Hence, it is possible to conclude that the microcontraction width is an important factor in the CFL manipulation.

By using soft lithography the best results was archived by the channel 6, a channel with a sequence of hyperbolic contractions. With the micromilling process the results appeared to be promising low cost alternative since the separation was partially achieved.

Both methods present good results and the new and low cost fabrication seems to be a good way to perform cell separation test.

However, the micromilling process need to be improved. The use of smaller tools and a resistant material can improve the precision of the geometries. In addition, a better understanding of the micromilling machine and softwares can reduce the possibility of human error.

References

Calejo, Joana Andreia Conceição. 2013. Desenvolvimento de Fluidos Bifásicos ao Sangue: Estudo Reológico, Escoamento em Microcanais e Simulações Numéricas. Bragança: s.n., 2013.

Duffy D C, McDonald J C, Schueller O J and Whitesides G M 1998 Rapid Prototyping of Microfluidic Systems in Poly(dimethylsiloxane) *Anal Chem* **70** 4974-4984

Faustino, Vera Luísa Carreira (2012) - The study of cell behaviour using biomedical microdevices. Bragança: Escola Superior de Tecnologia e Gestão. Dissertação de Mestrado em Tecnologia Biomédica.

Geschke, O., Klank, H., Telleman, P. (Eds.), Microsystem Engineering of Lab-on-a-Chip Devices. Wiley-vch (2008), 2nd edition, pp: 183-184

MicroChem, http://www.microchem.com/Prod-PMMA.htm, consultado a 10.10.2014.

Novais, Susana; Pinho, Diana; Bento, David; Pinto, Elmano; Yaginuma, Tomoko; Fernandes, Carla S.; Garcia, Valdemar; Pereira, Ana I.; Lima, José; Mujika, Maite Oliveira, Mónica S. N.; Dias, Ricardo P.; Arana, Sergio; Lima, R. (2014) - Cell-free layer (CFL) measurements in complex geometries: contractions and bifurcations. In Lima, Rui [et al.](eds.) Visualization and Simulation of Complex Flows in Biomedical Engineering. Lecture Notes in Computational Vision and Biomechanics. Springer. 12, p.119-132. ISBN 978-94-007-7768-2.

Novais, Susana Cristina Ribeiro. 2012. Desenvolvimento de um microdispositivo biomédico para a separação e deformação de eritrócitos. Bragança – s.n, 2012.

Pinho, Diana Margarida Domingues de. 2011. Determinação e Caracterização das

Trajetórias dos Glóbulos Vermelhos: Um Método Semi-Automático. Bragança: s.n,2011.

Pinto, Elmano Manuel Vieira (2012) - Estudo experimental de escoamentos fisiológicos em microcanais fabricados por xurografia. Bragança: Escola Superior de Tecnologia e Gestão. Dissertação de Mestrado em Tecnologia Biomédica.

Lima R, Wada S, Tanaka S, Takeda M, Ishikawa T, Tsubota K, Imai Y and Yamaguchi T 2008 In vitro blood flow in a rectangular PDMS microchannel: experimental observations using a confocal micro-PIV system *Biomedical Microdevices* **10** 153-167.

Leble V, Lima R, Dias R, Fernandes C, Ishikawa T, Imai Y and Yamaguchi T 2011 Asymmetry of red blood cell motions in a microchannel with a diverging and converging bifurcation *Biomicrofluidics* **5** 44120-4412015.

SetorVidreiro,http://www.setorvidreiro.com.br/o-que-procura/194/propriedades+fisicas+e+mecanicas+do+vidro, consultado 10.10.2014

Webopedia, http://www.webopedia.com/TERM/P/PMMA.html, consultado a 10.10.2014.

Wikipédia, http://pt.wikipedia.org/wiki/Acr%C3%ADlico_(pl%C3%A1stico)), consultado a 10.10.2014.

Appendix A

1. Positive Resist AZ® 9200

1.1. Lithography Procedure and Remarks

Test on more than one day of 06.2014 and 07.2014

Target thickness 15 µm – Thickness acquired 10-11 µm

Coat	**800 rpm for 15 s then 1500 rpm for 60 s**
Soft bake	105°C for 200 s
Rehydration	0 hours/2 hours /24 hours
Exposure	30s /150s / 50s /65 s
Development	. About 7 minutes

1.1.1. The time left for Rehydration prove to get some improvements to the side walls, and the air humidity influences a lot the time of rehydration;

1.1.2. Too much Exposure time destroys the smaller channels. The best result was with 65 s.

1.1.3. Development time depends on rehydration, for each try must have new developer.

Test on 08.07.2014

Target thickness 30 µm – Thickness acquired 20-30 µm

#1

. Coat	**. 500 rpm for 15 s then 1000 rpm for 60 s**
. Soft bake	. 100°C for 1m 50s
. Coat	. 500 rpm for 15 s then 1000 rpm for 60 s
. Soft bake	. 100°C for 3m 20s
. Rehydration	. 0
. Exposure	. 85s
. Development	. -/- visual

#2

Coat	**500 rpm for 15 s then 1000 rpm for 60 s**
Soft bake	100°C for 1m 50s
Coat	500 rpm for 15 s then 1000 rpm for 60 s
Softbake	100°C for 2m
Coat	500 rpm for 15 s then 1000 rpm for 60 s
Softbake	100°C for 3m 30s
Rehydratation	0
Exposure	100 s
Development	-/- visual

1.1.1. With the two layers I got a 33,3um of thickness.

1.1.2. The tree layers hasn´t exposure enough.

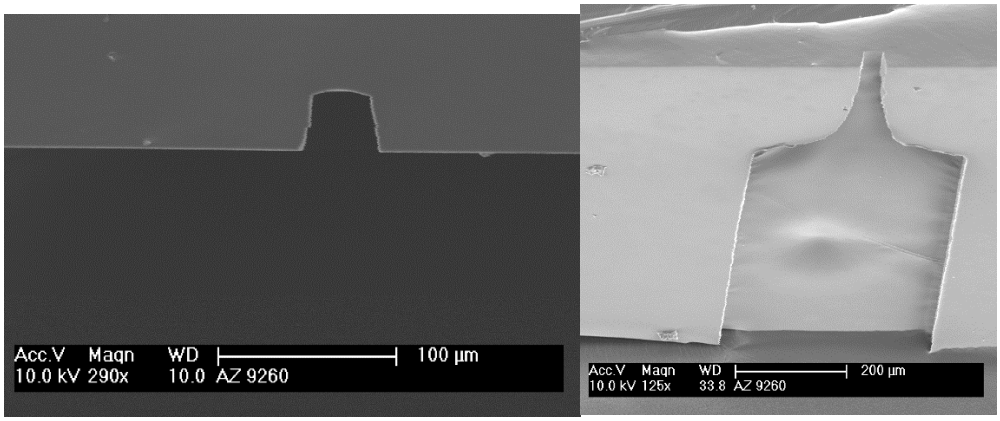

Figure 44 –Test on 8.07.2014 two layrers #1, results with SEM.

Test on 09.07.2014

Target thickness 40 µm – Thickness acquired >50 µm

#1

Coat	**500 rpm for 15 s then 1000 rpm for 60 s**
Soft bake	109°C for 1m 50s
Coat	500 rpm for 15 s then 1000 rpm for 60 s
Softbake	109°C for 2m 30s
Coat	500 rpm for 15 s then 1000 rpm for 60 s
Softbake	109°C for 4m 00s
Rehydratation	48h
Exposure	150 s
Development	-/- visual 8 m 00s

#2

Coat	**500 rpm for 15 s then 1000 rpm for 60 s**
Soft bake	100°C for 1m 50s
Coat	500 rpm for 15 s then 1000 rpm for 60 s
Softbake	100°C for 3m00s
Coat	500 rpm for 15 s then 1000 rpm for 60 s
Softbake	100°C for 6m 00s
Rehydratation	48h
Exposure	130 s
Development	-/- visual 16m30s

1.1.1. For preventing stress for the fast cooling, was preventing by cooling the wafer in a plastic surface;

1.1.2. For #1 I had good results but needs some improvements, the thickness was of 52,8 um ;

1.1.3. For #2 it took too long in the developer and the channels were destroyed.

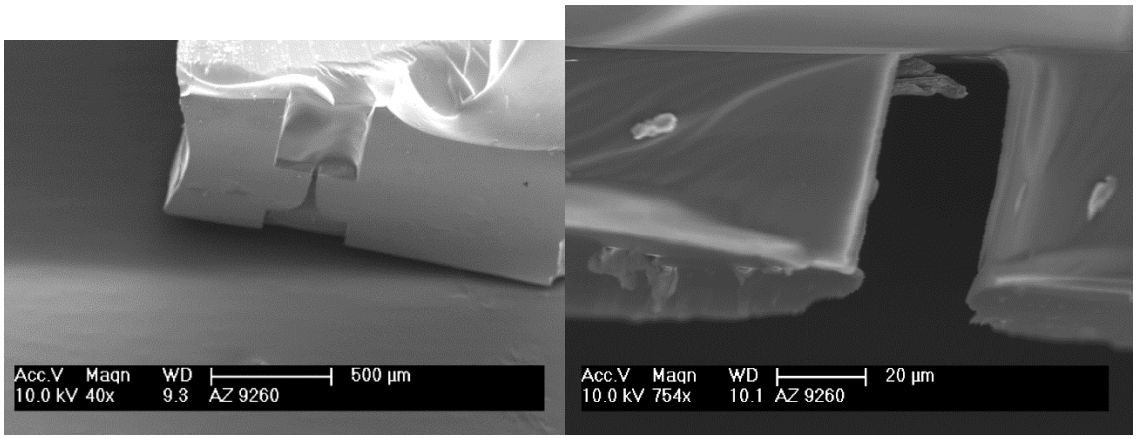

Figure 45 - Test on 9.07.2014 three layrer #1s, results with SEM.

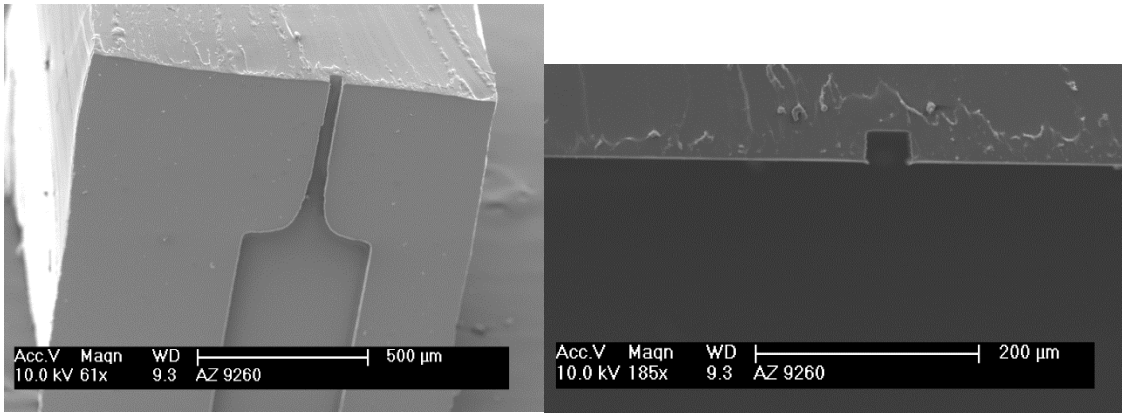

Figure 46 - Test with SU 8 for comparison.

Table 8 - Deeps obtained and Measured by the SEM microscope.

Figure 44	33.3 µm
Figure 45	52.8 µm
Figure 46	28.8 µm

Appendix B

1.1. Lithography Procedure

1. Materials you will need:
    a. Sample to put the resist (wafer for example);
    b. The resist;
    c. Tweezers;
    d. Sample holder;
    e. Hot Plate;
    f. Water;
    g. Developer (1/4);

Coat	**500 rpm for 15 s then 1000 rpm for 60 s**
Soft bake	100°C for 1m 50s
Coat	500 rpm for 15 s then 1000 rpm for 60 s
Soft bake	100°C for 3m 20s
Rehydration	For 60% of humidity is about one hour and 30 minutes
Exposure	85s
Development	-/- visual

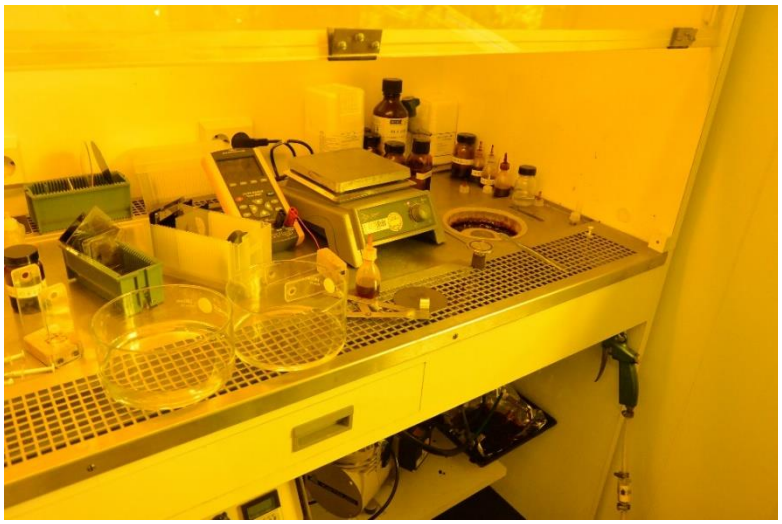

2. Turn on the spin coater, verify the velocities and turn on the hot plate and the vacuum bomb;
3. Clean the sample where you going to use the resist, the cleaning method depends on sample material;
    a. Si Wafers are cleaned in a circular motion starting in the middle with acetone.
4. Put the sample in the spin cotter, centralize it.
5. Dispense the resist on the sample, press the pedal of the spin coater to start working;
    a. The quantity should be similar to the image.

6. Now put the wafer with the resist on the hotplate, counting the time;

7. Give some time so the resist can rehydrate;
8. While waiting turn on the vacuum pump for the lithography machine and the lithography machine;

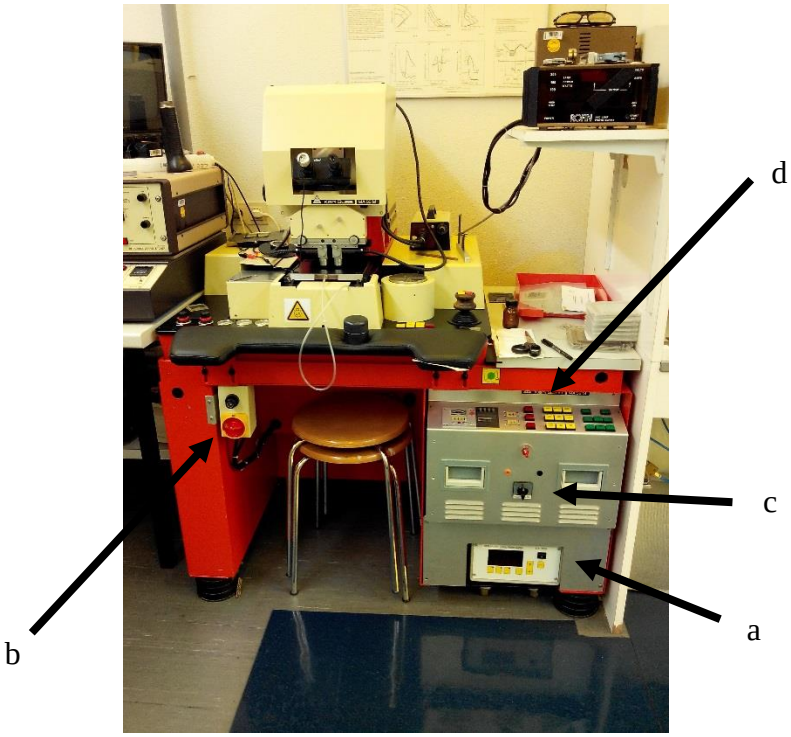

a. Turn to 1 the black button, then press start;
b. Turn the red lever to one, wait between 1 to 2 minutes;
c. Black lever to 1;
d. Press “W/O loader”, then prepare the mask and click “Mask Load”.

9. Exposure it;
    a. Position the sample;

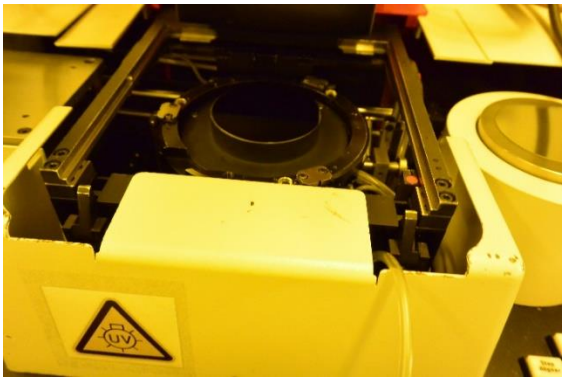

    b. Put the mask into place and press “Mask Clamp” give it time to position;

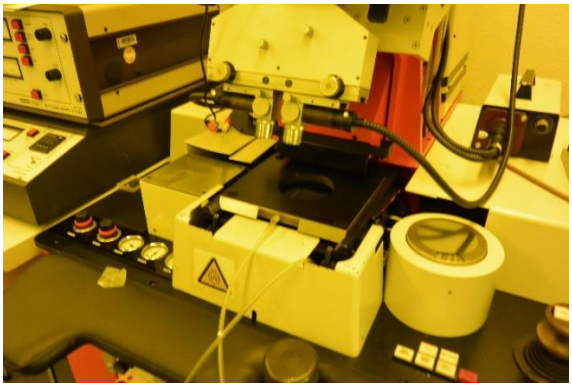

    c. Press “Start Aligner” and wait a few seconds;
        i. Substrate automatically moves to the top;
        ii. Balancing substrate wedge error mask;
        iii. The substrate moves in adjusting distance.
    d. Then “Align” (Approach contact, exposure lights)
    e. Press “Exposure”;
    f. After the exposure, press “Mask Clamp”, remove the mask from the position and then remove the wafer.
10. With the help of the wafer holder, lock the wafer and very carefully dip it in the developer, move it in every direction, to always have new developer in the wafer. This time can change for many reasons, observe and remove the sample when all the resist that´s supposed to be removed as been.
11. Wash the sample on the water;
12. Blow it up, to dry it, from the top to bottom;
13. Keep the final product.